



Functional Validation of *CLDN* Variants Identified in a Neural Tube Defect Cohort Demonstrates Their Contribution to Neural Tube Defects

Amanda I. Baumholtz^{1,2}, Patrizia De Marco³, Valeria Capra⁴ and Aimee K. Ryan^{1,2,5*}

¹ Department of Human Genetics, McGill University, Montreal, QC, Canada, ² The Research Institute of the McGill University Health Centre, Montreal, QC, Canada, ³ Laboratorio di Neurogenetica e Neuroscienze, Istituto Giannina Gaslini, Genoa, Italy, ⁴ U.O. Neurochirurgia, Istituto Giannina Gaslini, Genoa, Italy, ⁵ Department of Pediatrics, McGill University, Montreal, QC, Canada

OPEN ACCESS

Edited by:

Ioannis Dragatsis,
The University of Tennessee Health
Science Center (UTHSC),
United States

Reviewed by:

Lee Niswander,
University of Colorado Boulder,
United States
Laura Mitchell,

The University of Texas Health
Science Center at Houston,
United States
Michael Koval,
Emory University, United States

*Correspondence:

Aimee K. Ryan
aimee.ryan@mcgill.ca

Specialty section:

This article was submitted to
Neurogenomics,
a section of the journal
Frontiers in Neuroscience

Received: 23 February 2020

Accepted: 29 May 2020

Published: 14 July 2020

Citation:

Baumholtz AI, De Marco P,
Capra V and Ryan AK (2020)
Functional Validation of *CLDN*
Variants Identified in a Neural Tube
Defect Cohort Demonstrates Their
Contribution to Neural Tube Defects.
Front. Neurosci. 14:664.
doi: 10.3389/fnins.2020.00664

Neural tube defects (NTDs) are severe malformations of the central nervous system that affect 1–2 individuals per 2,000 births. Their etiology is complex and involves both genetic and environmental factors. Our recent discovery that simultaneous removal of *Cldn3*, *-4*, and *-8* from tight junctions results in cranial and spinal NTDs in both chick and mouse embryos suggests that claudins play a conserved role in neural tube closure in vertebrates. To determine if claudins were associated with NTDs in humans, we used a Fluidigm next generation sequencing approach to identify genetic variants in *CLDN* loci in 152 patients with spinal NTDs. We identified eleven rare and four novel missense mutations in ten *CLDN* genes. *In vivo* validation of variant pathogenicity using a chick embryo model system revealed that overexpression of four variants caused a significant increase in NTDs: *CLDN3* A128T, *CLDN8* P216L, *CLDN19* I22T, and E209G. Our data implicate rare missense variants in *CLDN* genes as risk factors for spinal NTDs and suggest a new family of proteins involved in the pathogenesis of these malformations.

Keywords: claudin, tight junction, neural tube defects, myelomeningocele, fluidigm

INTRODUCTION

Neural tube defects (NTDs) [MIM: 182940] are a group of congenital central nervous system malformations that affect the brain and spinal cord, caused by failure of neural tube closure during embryogenesis. They have a complex etiology involving both genetic and environmental factors. The two most common forms are the cranial defect, anencephaly, and the spinal defect, myelomeningocele (spina bifida). A third rare form of open NTDs, craniorachischisis, occurs when the neural tube fails to close along the entire length of the body axis. NTDs are the second most common birth defect with a varying incidence, affecting 1–2 per 2,000 pregnancies in North America post-folic acid fortification, and as high as 20 per 1,000 births in certain regions of China (Chen et al., 2009). Approximately 300,000 newborns affected by these defects are born annually (Zaganjor et al., 2016). Thus, there is an urgent need to better understand the underlying pathogenic mechanisms of NTDs, particularly those not prevented by folic acid fortification.

Neural tube closure, which occurs during the fourth week of human gestation, is divided into four distinct phases (Wang et al., 2019). First, a subset of medial ectodermal cells is induced to differentiate into neural progenitors, which form the neural plate. Next, the neural plate undergoes convergent extension, which leads to its mediolateral narrowing and anterior–posterior extension.

This is followed by apical constriction of midline cells to form the median hinge point, which allows the neural plate to bend at the midline and the lateral edges of the neural plate to elevate and become the neural folds. Finally, the lateral edges of the neural folds meet at the dorsal midline where they fuse to generate a closed neural tube and a contiguous overlying layer of surface ectoderm.

A defect in any of these phases of neural tube closure will result in a NTD. Defects in convergent extension, which is regulated by the non-canonical Wnt/planar cell polarity (PCP) pathway, result in NTDs due to the fact that the lateral edges of the neural folds never come in close enough proximity to fuse. Many animal models with mutations in PCP components develop NTDs due to aberrant convergent extension movements (Greene et al., 1998; Goto and Keller, 2002; Wallingford and Harland, 2002; Curtin et al., 2003; Wang J. et al., 2006; Wang Y. et al., 2006; Ybot-Gonzalez et al., 2007; Paudyal et al., 2010) and rare and novel missense mutations in PCP genes are risk factors for NTDs in humans (Kibar et al., 2009, 2011; Lei et al., 2010, 2019; Bosoi et al., 2011; Allache et al., 2012; De Marco et al., 2012, 2013; Robinson et al., 2012). The PCP pathway is one of the few candidate pathways identified in animal models whose human homologs have been shown to contribute to risk of human NTDs. Formation of the hinge points requires RhoA/ROCK-mediated actin-myosin contraction of the apical surface of neural plate cells (Kinoshita et al., 2008; Rolo et al., 2009; Escuin et al., 2015).

We recently discovered that claudins act upstream of the PCP and RhoA/ROCK signaling pathways to regulate cell shape changes and tissue movements during neural tube morphogenesis (Baumholtz et al., 2017). Indeed, simultaneous removal of *Cldn3*, *-4*, and *-8* from tight junctions causes open NTDs in both chick and mouse embryos (Baumholtz et al., 2017). Claudins comprise a family of integral tight junction proteins with ~24 unique members in vertebrates. They have four transmembrane domains, two extracellular loops, and cytoplasmic N- and C-termini. The first extracellular loop contains charged amino acids that determine the ion and size selectivity of the tight junction paracellular barrier (Katahira et al., 1997; Hamazaki et al., 2002; Simard et al., 2005; Robertson et al., 2007; Baumholtz et al., 2017; Nakamura et al., 2019). The second extracellular loop participates in *trans*-interactions with claudin molecules in apposing cells, and in *cis*-interactions with other claudins in the same cell (Piontek et al., 2008; Suzuki et al., 2014). The transmembrane domains also participate in *cis*-oligomerization (Rossa et al., 2014). Together, these interactions constitute the backbone of tight junction strands and prevent the mixing of apical and basolateral proteins (Krause et al., 2015). The claudin cytoplasmic C-terminal tail has a conserved PDZ-binding domain that interacts with adaptor proteins at the tight junction cytoplasmic plaque, thereby linking the tight junction to the actin cytoskeleton and intracellular signaling events (Van Itallie et al., 2013; Fredriksson et al., 2015; Baumholtz et al., 2017). The C-terminal domain also contains numerous phosphorylation sites that can influence protein interactions at the tight junction cytoplasmic plaque (Tanaka et al., 2005; Ikari et al., 2006).

Given the importance of claudins in neural tube closure in chick and mouse, we tested our hypothesis that mutations in

CLDN genes are risk factors for human NTDs by screening a cohort of 152 open spinal NTD patients for rare and novel non-synonymous *CLDN* variants. We identified 11 rare and four novel missense variants in 10 *CLDN* genes. We then tested the functional consequences of the *CLDN* variants by transfection of HEK293 or MDCK II cells to determine if the variant protein localized to the tight junction and then by overexpressing the variants in chick embryos to determine if the variants caused defects in neural tube closure. Our data suggest that rare missense mutations in *CLDN* genes are risk factors for human NTDs.

SUBJECTS AND METHODS

Neural Tube Defect Cohort

The studies involving human participants were reviewed and approved by IRCCS Istituto Giannina Gaslini (Protocol number: IGG-VACA, 18 September 2011) and the Research Institute of the McGill University Health Centre (Protocol number: 14-444-PED). Written informed consent to participate in this study was provided by the participants and/or their legal guardian/next of kin. The patient cohort consisted of 152 unrelated individuals with myelomeningocele, who were recruited at the Spina Bifida Center of the Gaslini Hospital in Genova, Italy, between the period of 2006–2017. The age of patients ranged from 3 to 20 years, with the mean age being 9.6 years. The female/male ratio was 1.2. All participants were Italians with antecedents from all parts of the country. The majority of these individuals were of European ancestry, although some individuals were of Hispanic or African ancestry. Upon entering the study, individuals were re-evaluated by a clinical geneticist and diagnosis was made on the basis of MRI, X-ray images and clinical records, according to previously described criteria (Rossi et al., 2004). The study group includes individuals who were previously analyzed for mutation of PCP genes (Kibar et al., 2009, 2011; Bosoi et al., 2011; Allache et al., 2012; De Marco et al., 2012, 2013; Robinson et al., 2012).

Next-Generation DNA Sequencing

Genomic DNA was isolated from blood samples using the QIAamp DNA blood kit according to the manufacturer's protocol (Qiagen, Milan, Italy). The genomic sequence of *CLDNs* was determined using the UCSC Genome Browser assembly ID hg19 (*CLDN1*: RefSeq NG_021418.1 [MIM: 607626]; *CLDN2*: RefSeq NG_016445.1, *CLDN3*: RefSeq NG_012023.1; *CLDN4*: RefSeq NG_012868.1; *CLDN5*: GenBank NC_000022.10; *CLDN6*: GenBank NC_000016.9; *CLDN7*: GenBank NC_000017.10; *CLDN8*: RefSeq NG_050758.1; *CLDN9*: NC_000016.9; *CLDN10*: RefSeq NG_047100.1 [MIM: 617671]; *CLDN11*: GenBank NC_000003.11; *CLDN12*: GenBank NC_000007.13; *CLDN14*: GenBank NC_000021.8 [MIM: 614035]; *CLDN15*: GenBank NC_000007.13; *CLDN16*: RefSeq NG_008149.1 [MIM: 248250]; *CLDN17*: GenBank NC_000021.8; *CLDN18*: GenBank NC_000003.11; *CLDN19*: RefSeq NG_008993.1 [MIM: 248190]; *CLDN20*: RefSeq NG_027528.2; *CLDN21*: RefSeq NG_051586.1; *CLDN22*: RefSeq NG_051586; *CLDN23*: GenBank NC_000008.10; *CLDN24*: RefSeq NG_051586.1; *CLDN25*: GenBank NC_000011.9). DNA was then processed by

microfluidic polymerase chain reaction (PCR) using a custom Fluidigm Access Array, followed by next-generation sequencing on an Illumina MiSeq platform at the McGill University and Genome Quebec Innovation Center (Montreal, QC, Canada). Briefly, 92 custom pairs of primers were designed to amplify ~300 bp fragments of the coding exons of the 24 human claudin genes (**Supplementary Table S1**). Primer sets were validated using a standard PCR protocol to ensure that they amplified a single fragment of the expected size, and selected amplicons were validated by Sanger sequencing. The amplicons from the array were pooled and the resulting pools were multiplexed and sequenced using the Illumina MiSeq. Reads were processed and aligned to the human genome (UCSC hg19, NCBI build 37) by Genome Quebec. Aligned and processed BAM files were used to manually identify variants using the Integrative Genomics Viewer version 2.3 (Robinson et al., 2011, 2017; Thorvaldsdottir et al., 2013). Variants with alternative allele frequencies of 30% or greater were selected for further analysis.

Sanger Sequencing of CLDN3

The single *CLDN3* coding exon was amplified by PCR using a single primer pair (**Supplementary Table S2**) and subjected to Sanger sequencing at the McGill University and Genome Quebec Innovation Centre (Montreal, QC, Canada). Samples were sequenced in both directions using specific forward and reverse primers. The *CLDN3* variants were confirmed by repeating the PCR and re-sequencing from a single direction.

Bioinformatics

Variants were annotated according to the HGVS nomenclature¹. The Exome Variant Server (EVS² (Exome Variant Server, 2020) and Genome Aggregation Database v2.1.1 (gnomAD³ (Karczewski et al., 2020) public databases were queried for the presence and incidence of the variants identified in *CLDN1-25*. Rare variants were defined as having a minor allele frequency (MAF) < 1% in these databases and novel variants were defined as those not present in these databases. The potential pathogenic effect of the identified mutations on protein function was predicted using three software programs: Polymorphism Phenotyping v2 (PolyPhen-2⁴; Adzhubei et al., 2010), Sorting Intolerant from Tolerant (SIFT⁵) (Ng and Henikoff, 2003) and MutationTaster⁶ (Schwarz et al., 2010). Multiple alignments of the CLDN proteins were done using the Clustal Omega program⁷. Localization of the variants in protein domains was assessed by Uniprot⁸. Predicted phosphorylation sites in CLDN proteins were identified using NetPhos 3.1⁹ (Blom et al., 1999).

¹<https://varnomen.hgvs.org/>

²<http://evs.gs.washington.edu/EVS/>

³<https://gnomad.broadinstitute.org/>

⁴<http://genetics.bwh.harvard.edu/pph2/>

⁵<http://sift.bii.a-star.edu.sg/>

⁶<http://www.mutationtaster.org/>

⁷<https://www.ebi.ac.uk/Tools/msa/clustalo/>

⁸<https://www.uniprot.org/>

⁹<http://www.cbs.dtu.dk/services/NetPhos/>

DNA Resequencing of CLDNs

Rare and novel missense variants were validated by Sanger sequencing. Primers flanking the coding exons of *CLDN3* (RefSeq NM_001306.3), *CLDN4* (RefSeq NM_001305.4), *CLDN6* (RefSeq NM_021195.4), *CLDN8* (RefSeq NM_199328.2), *CLDN9* (RefSeq NM_020982.3), *CLDN14* (RefSeq NM_144492.2), *CLDN16* (RefSeq NM_006580.3), *CLDN18* (RefSeq NM_001002026.2), *CLDN19* (RefSeq NM_148960.2), *CLDN23* (RefSeq NM_194284.2), *CLDN24* (RefSeq NM_001185149.1) were used to amplify the coding region by polymerase chain reaction (**Supplementary Table S2**). Amplicons were subjected to Sanger sequencing at the McGill University and Genome Quebec Innovation Centre (Montreal, QC, Canada).

Generation of Claudin Wild-Type and Mutant Constructs

The full-length human wild-type and variant sequences for claudins encoded by a single exon (*CLDN3*, 4, 6, and 24) were amplified from genomic DNA of NTD patients by PCR and cloned into the pSCA vector using the Stratagene PCR cloning kit (Agilent Technologies, Santa Clara, CA, United States). pMXs-Puro-CLDN18 was a gift from Axel Hillmer (Addgene plasmid #69466) (Yao et al., 2015) and used as a template to clone full-length *CLDN18* into pSCA. *CLDN16* p.N223S, *CLDN18* p.V88I and *CLDN19* p.I22T were introduced in the pSCA-claudin constructs by site-directed mutagenesis using the Stratagene QuikChange II Site-Directed Mutagenesis kit according to manufacturer's directions (Agilent Technologies, Santa Clara, CA, United States). *CLDN19* p.E209G was created by PCR using a reverse primer containing the mutation and pSCA-HCLDN19 as a template. Sequence identity of cDNA clones was confirmed by sequencing at the McGill University and Genome Quebec Innovation Centre (Montreal, QC, Canada). Wild-type and variant constructs were then cloned into the pCanHA3 and pMES-IRES-GFP expression plasmids. Primer sequences used for mutagenesis reactions are shown in **Supplementary Table S3**.

Immunolocalization of Ectopically Expressed Claudins

HEK293 and MDCK II cells were grown in Dulbecco's Modified Eagle's Medium supplemented with 10% fetal bovine serum and antibiotics. HEK293 cells were plated on coverslips in a 24-well plate and reached 70–90% confluence the day of the transfection experiments. pMES or pCanHA3 expression vectors encoding wild-type or variant claudins were transiently transfected into HEK293 cells using Lipofectamine LTX (Invitrogen) in a 1:1 DNA-reagent ratio using 500 ng of plasmid DNA per well. MDCK II cells were transfected in suspension using Polyjet (FroggaBio) in a 4:1 DNA-reagent ratio using 500 ng plasmid per well and plated on coverslips in a 24-well plate at 70% confluency. HEK293 and MDCK II cells were cultured for 24 h after transfection. After rinsing with PBS, cells were fixed with 10% trichloroacetic acid or 4% PFA for 10 min at 4°C, blocked with 10% normal goat serum in 0.3% Triton X-100 in PBS and then incubated with primary antibody for 1 h at room temperature. Primary antibodies used were Cldn3 and 16 (Abcam, Cambridge, United Kingdom, 1:100),

Cldn8 (Invitrogen, Carlsbad, CA, United States, 1:100), ZO-1 (Invitrogen, 1:100, Carlsbad, CA, United States), and HA (Invitrogen, Carlsbad, CA, United States, 1:100). Antibodies were detected with Alexa Fluor® 488 conjugated goat anti-rabbit IgG and Alexa Fluor® 594 conjugated goat anti-mouse IgG (Molecular Probes). Slides were coverslipped with SlowFade Gold Antifade kit (Molecular Probes), which contained DAPI to enable visualization of the nuclei, and imaged using a laser scanning confocal microscope (LSM780, Leica, Germany).

Overexpression Assay in the Chick Embryo

CLDN-IRES-GFP pMES expression vectors (5 µg/µl) were injected into the space between the vitelline membrane and the epiblast of HH4 embryos cultured *ex ovo* on agar-albumen plates using a Narishige IM 300 microinjector, and then electroporated using a Protech CUY21SC square electroporator (five 3 V/50 ms pulses at 500 ms intervals). Manipulated embryos were cultured at 39.5°C until HH11-13 and then scored for defects in neural tube closure and convergent extension. Brightfield and GFP images of electroporated embryos were taken using a Leica M205FA dissecting microscope and Leica DFC450C camera with Leica Application Suite X software. Only embryos with GFP expression in neural and non-neural ectoderm cells were included for phenotype evaluation.

Assessment of Axial Length

Dorsal images of HH12 embryos (somite stage 15–17) were photographed using a Leica M125 dissecting microscope and imported into ImageJ software. Axial length was measured from the tip of the forebrain to the tip of the tail bud.

Whole Mount *in situ* Hybridization

Whole-mount *in situ* hybridization was performed as previously described (Collins and Ryan, 2011). Embryos were photographed using a Leica M125 dissecting microscope with Infinity Capture software v5.0.2 (Lumenera Corp.). Paraffin-embedded embryos were sectioned and photographed using a Zeiss Axiophot compound microscope and AxioCamMRC camera with Axiovision v4.7.1.0 software.

Histology

Embryos were fixed overnight in 4% paraformaldehyde, dehydrated in a graded ethanol series and embedded in paraffin wax. Seven-micron sections were stained using Mayer's hematoxylin solution and Eosin Y (both Sigma). Images were captured on a Leica DM6000B upright microscope equipped with a DFC450C camera.

Statistical Analyses

Anterior–posterior length of embryos overexpressing variant *CLDN* constructs compared to wild-type *CLDN* was analyzed by Mann–Whitney *U*-test. To assess the ability of *CLDN* variants to affect neural tube closure in our gain-of-function experiments, a Chi-square test was performed comparing the proportion of open NTDs between embryos overexpressing *CLDN* variants

compared to wild-type *CLDN* or control empty plasmid. All statistics were computed using GraphPad Prism software.

RESULTS

NTD Patients Have Rare and Novel *CLDN* Variants

To examine the association of *CLDN* mutations in the etiology of human NTDs, we sequenced the coding region of the 24 human *CLDN* genes in 152 patients with open spinal NTDs (myelomeningocele) by targeted next generation sequencing. Recent publications of large population sequencing data provide an opportunity to characterize with accuracy and precision the frequency distributions of rare disease-causing alleles. Since we did not have an adequate control group for size and for ethnicity, we decided to use the Exome Variant Server (EVS) (Exome Variant Server, 2020) that catalogs whole exome sequencing data of 6503 unrelated European and African Americans, and the gnomAD database (Karczewski et al., 2020) that provides variants from 125,748 exomes and 15,708 genomes of unrelated individuals for making inferences on the overall role of *CLDN* variants. Importantly, neither database contains individuals with severe congenital anomalies. The EVS database contains healthy controls and extremes of specific adult onset traits and/or diseases, including blood pressure, early onset myocardial infarction and stroke, and lung disease. In the gnomAD database, individuals affected by severe pediatric disease, and their first-degree relatives, were removed. Thus, neither database contains individuals with myelomeningocele open NTDs, supporting their use as appropriate control populations for our study cohort. The individuals in these databases are adults, and therefore, deleterious variants for any gene that have the potential to contribute to conditions associated with early mortality may be underrepresented. To date, gnomAD is the largest and most comprehensive source of genetic information of individuals of different ethnic backgrounds and similar to our cohort, the largest ethnicity represented is non-Finnish Europeans. However, neither database provides precise ancestry information. Another potential limitation to the database is that the sequencing data are derived from different exome capture approaches and sequencing platforms, which leads to variation in coverage between individuals and across sites. While this may impact the exact allele frequency, the large number of individuals that have been analyzed allows us to distinguish between common, rare and novel variants. With respect to our own data, we only considered variants where the alternate allele was present in at least 30% of the sequencing reads.

We found 69 variants in total: 37 synonymous single nucleotide polymorphisms (SNPs) and 32 non-synonymous missense variants. Of the missense variants, 17 were common (Table 1), 11 were rare [minor allele frequency (MAF) < 1%] and four were not found in the dbSNP (Sherry et al., 2001), EVS (Exome Variant Server, 2020), or gnomAD (Karczewski et al., 2020) publicly available databases (Table 2). All rare and novel missense variants in *CLDN*s were confirmed by Sanger sequencing, except for the *CLDN24* p.E161K as there was no

TABLE 1 | Common non-synonymous variants in the coding sequence of *CLDN1-25*.

Gene	Accession number	Nucleotide change	Amino acid change	Allele frequency count/ (%) NTD cases	Allele frequency count/ (%) gnomAD	Allele frequency count/ (%) EVS
<i>CLDN6</i>	NC_000016.9	c.388G > C	p.V130L	1 (0.33)	3938 (1.396)	161 (1.2388)
		c.427A > G	p.I143V	126 (41.45)	101902 (36.36)	5010 (38.5741)
<i>CLDN7</i>	NC_000017.10	c.590T > C	p.V197A	212 (69.74)	185318 (65.8)	3944 (30.3245)
<i>CLDN8</i>	NG_050758.1	c.290T > C	p.M97T	1 (0.33)	1608 (0.5687)	229 (1.7607)
		c.385A > G	p.T129A	20 (6.57)	14671 (5.192)	1103 (8.4807)
		c.451T > C	p.S151P	76 (25)	84042 (29.83)	8008 (38.4284)
<i>CLDN14</i>	NC_000021.8	c.11C > T	p.T4M	14 (4.60)	4972 (2.738)	402 (4.3946)
<i>CLDN16</i>	NG_008149.1	c.C166del	p.A56LfsTer16	116 (38.16)	54308 (19.24)	0 (0)
		c.166C > G	p.A56P	116 (38.16)	54311 (19.24)	0 (0)
<i>CLDN17</i>	NC_000021.8	c.244G > A	p.A82T	31 (10.20)	26892 (9.437)	892 (6.8584)
<i>CLDN18</i>	NC_000003.11	c.445A > T	p.M149L	19 (6.25)	32284 (11.42)	1398 (10.7489)
<i>CLDN19</i>	NG_008993.1	c.599G > A	p.R200Q	2 (0.66)	3396 (1.508)	148 (1.1422)
<i>CLDN20</i>	NG_027528.2	c.281G > A	p.G94E	2 (0.66)	3977 (1.406)	119 (0.915)
<i>CLDN23</i>	NC_000008.10	c.628G > A	p.V210M	28 (9.21)	26931 (13.32)	941 (7.8521)
<i>CLDN24</i>	NG_051586.1	c.52C > T	p.L18F	222 (73.03)	208872 (76.22)	N/A
		c.391A > G	p.I131V	2 (0.66)	3227 (1.163)	N/A
		c.621G > C	p.Q207H	55 (18.09)	43187 (23.47)	N/A

TABLE 2 | Novel and rare non-synonymous variants in the coding sequence of *CLDN1-25*.

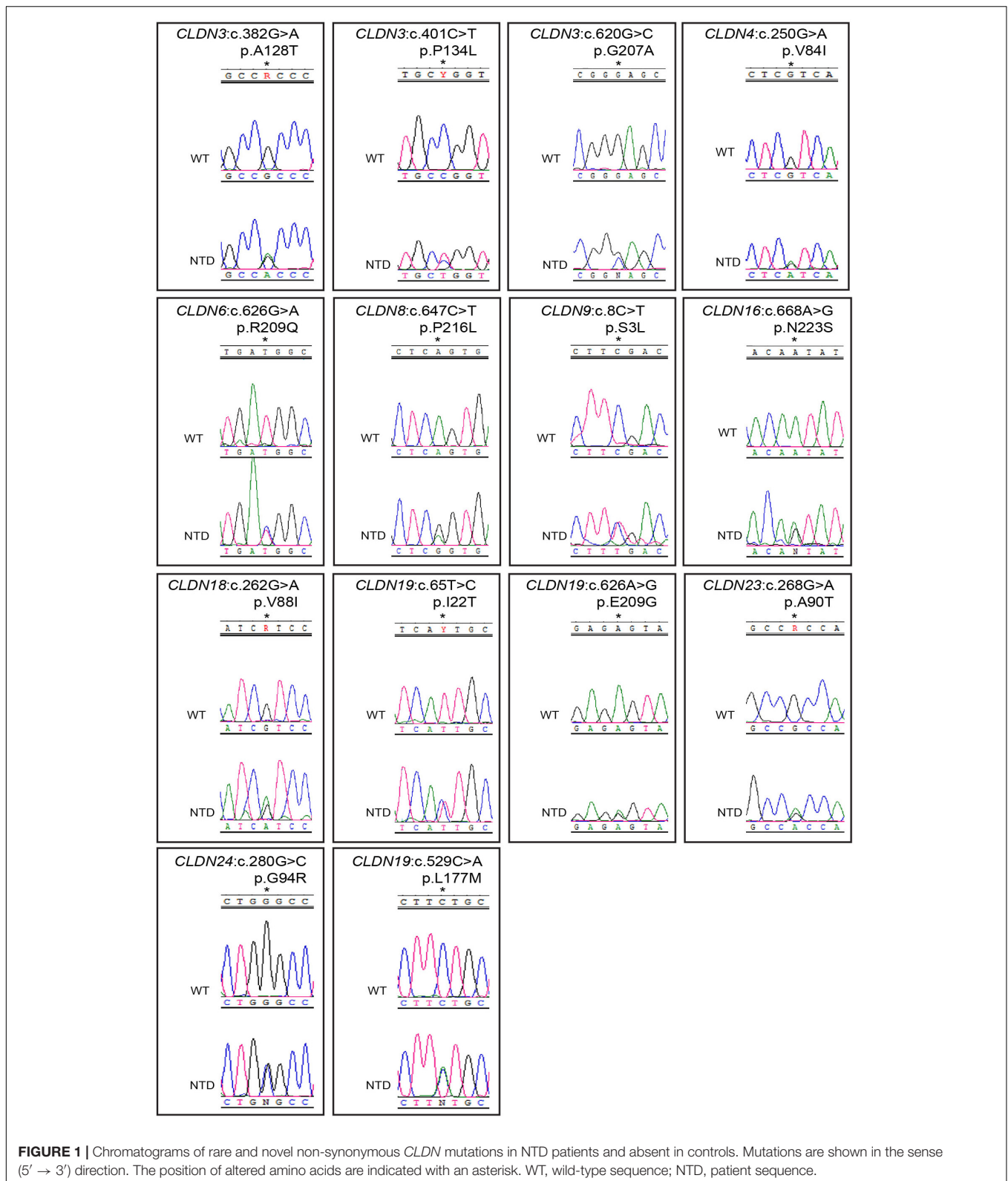
Gene	Accession number	Nucleotide change	Amino acid change	Fluidigm allele frequency	Fluidigm read depth	Allele frequency count/ (%) NTD cases	Allele frequency count/ (%) gnomAD	Allele frequency count/ (%) EVS	Ethnicity
<i>CLDN3</i>	NG_012023.1	c.382G > A	p.A128T	N/A	N/A	3 (1.0)	0 (0)	0 (0)	European
		c.401C > T	p.P134L	N/A	N/A	2 (0.7)	1253 (0.4519)	63 (0.484)	European
		c.620G > C	p.G207A	N/A	N/A	1 (0.3)	0 (0)	0 (0)	European
<i>CLDN4</i>	NG_012868.1	c.250G > A	p.V84I	49%	48282	1 (0.3)	6 (0.002388)	1 (0.0077)	European
<i>CLDN6</i>	NC_000016.9	c.626G > A	p.R209Q	54%; 53%	543; 4993	2 (0.7)	299 (0.1406)	20 (0.1539)	European, Hispanic
<i>CLDN8</i>	NG_050758.1	c.647C > T	p.P216L	55%	1293	1 (0.3)	906 (0.3204)	151 (1.161)	African
<i>CLDN9</i>	NC_000016.9	c.8C > T	p.S3L	48%	844	1 (0.3)	311 (0.1114)	3 (0.0231)	European
<i>CLDN16</i>	NG_008149.1	c.668A > G	p.N223S	40%	50	1 (0.3)	90 (0.03181)	3 (0.0231)	European
<i>CLDN18</i>	NC_000003.11	c.262G > A	p.V88I	51%; 50%	35; 1077	2 (0.7)	568 (0.2009)	22 (0.1692)	European
<i>CLDN19</i>	NG_008993.1	c.65T > C	p.I22T	50%	3067	1 (0.3)	117 (0.05170)	8 (0.0616)	European
		c.626A > G	p.E209G	43%	2407	1 (0.3)	17 (0.007741)	0 (0)	European
<i>CLDN23</i>	NC_000008.10	c.268G > A	p.A90T	57%	54	1 (0.3)	1225 (0.4753)	59 (0.4624)	European
<i>CLDN24</i>	NG_051586.1	c.280G > C	p.G94R	52%	787	1 (0.3)	0 (0)	N/A	European
		c.481G > A	p.E161K	32%	964	1 (0.3)	1 (0.0004875)	N/A	European
		c.529C > A	p.L177M	40%	1762	1 (0.3)	0 (0)	N/A	European

genomic DNA remaining for this patient (**Figure 1**). All rare and novel missense variants discovered were heterozygous and most were found in a single patient with the exception of *CLDN3* p.A128T that was found in three unrelated patients and *CLDN3* p.P134L, *CLDN6* p.R209Q and *CLDN18* p.V88I that were each found in two unrelated patients (**Table 2**). No NTD patient was a carrier of a rare or novel missense mutation in more than one *CLDN* gene. Sixteen of the 20 patients with a novel or rare mutation in a *CLDN* gene were previously analyzed for mutations in PCP genes (Kibar et al., 2009, 2011; Bosoi et al., 2011; Allache et al., 2012; De Marco et al., 2012, 2013; Robinson et al., 2012). A mutation in a PCP gene was identified in 4 of

these 16 patients (**Table 3**); mutations in PCP genes have been associated with NTDs.

Predictions of the Impact of Rare and Novel Variants on Protein Function

Rare variants are known to be causal genetic factors for complex diseases (Manolio et al., 2009; Bruel et al., 2017) and rare missense variants have been associated with NTDs in humans (Li et al., 2018). Therefore, we focused our analysis on the 4 novel and 11 rare missense variants. PolyPhen-2 (Adzhubei et al., 2010), SIFT (Ng and Henikoff, 2003), and



MutationTaster (Schwarz et al., 2010) were used to evaluate the potential pathogenic effect of each variant based on the degree of evolutionary conservation of the affected residue and the nature

of the amino acid replacement and its possible impact on protein function and localization (**Supplementary Table S4**). 10 of the 15 rare and novel missense variants were predicted to be pathogenic

TABLE 3 | Patients carrying mutations in a *CLDN* gene and core PCP gene.

CLDN gene	CLDN variant	PCP gene	PCP variant	Ethnicity
<i>CLDN3</i>	p.A128T	<i>CELSR1</i>	p.G934R	European
<i>CLDN6</i>	p.R209Q	<i>VANGL1</i>	p.C145C	European
<i>CLDN16</i>	p.N223S	<i>DVL2</i>	p.T535I	European
<i>CLDN23</i>	p.A90T	<i>DVL2</i>	p.T535I	European

with the potential to impact protein function by at least one of these tools. These variants are described below and were the focus of our functional studies.

The MAF (%) of these variants in the gnomAD and EVS databases, respectively, were 0.4519 and 0.4845 for *CLDN3* p.P134L, 0.3204 and 1.161 for *CLDN8* p.P216L, 0.1114 and 0.0231 for *CLDN9* p.S3L, 0.03181 and 0.0231 for *CLDN16* p.N223S, 0.2009 and 0.1692 *CLDN18* p.V88I, 0.0517 and 0.0616 for *CLDN19* p.I22T, 0.007741 and not reported for *CLDN19* p.E09G, and 0.0004875 and not reported for *CLDN24* p.E161K (Table 2). With the exception of the *CLDN8* p.P216L variant, ethnicity did not impact the MAF such that it would change the categorization of a variant as common versus rare (<1%). In the gnomAD database the MAF was 10-fold higher among Africans (MAF = 3.3%), and in the EVS database the MAF was 3.43% for African Americans and 0 for European Americans. The amino acid residues *CLDN3* p.P134, *CLDN16* p.N223, *CLDN18* p.V88, *CLDN19* p.E209, and *CLDN24* p.E161 are evolutionarily conserved, while *CLDN8* p.P216, *CLDN9* p.S3, and *CLDN19* p.I22 are conserved in mammals.

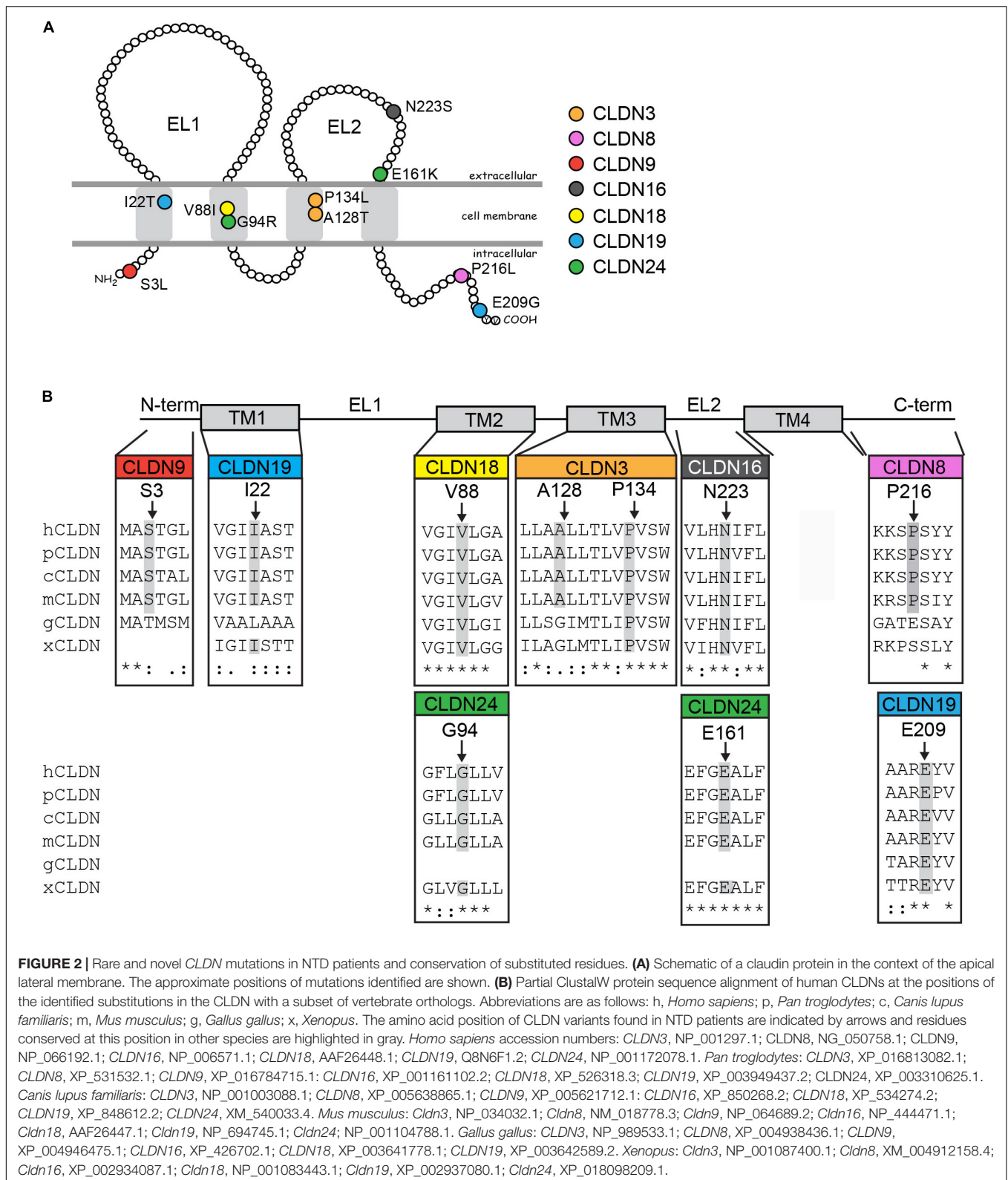
These variants are located throughout the different claudin protein domains (Figure 2). *CLDN9* p.S3L localizes to the N-terminus. The amino acid substitution of serine to leucine results in loss of a putative phosphorylation site as predicted by NetPhos3.1 and could alter protein structure. The *CLDN3* p.P134L, *CLDN18* p.V88I, and *CLDN19* p.I22T variants are located in transmembrane domains. The amino acid substitution proline to leucine results in loss of a bulky side chain, which could alter the structure of the CLDN3 protein. In fact, a recent study showed that the cyclic structure of proline's side chain at position 134 of CLDN3 causes bending of the third transmembrane domain affecting Cldn-Cldn *cis*-interactions and loss of a cyclic side chain by alanine or glycine substitution causes a change in CLDN3 protein conformation (Nakamura et al., 2019). Substituting valine with isoleucine in CLDN8 does not change the hydrophobic characteristics of the residue, although isoleucine has a bulky side chain that could interfere with protein-protein interactions. In CLDN19, replacement of isoleucine with threonine results in loss of hydrophobicity at this position and may affect the ability of the transmembrane domain to insert into the plasma membrane. *CLDN19* p.I22T also introduces a putative phosphorylation site as predicted by NetPhos3.1. *CLDN16* p.N223S and *CLDN24* p.E161K change residues in the second extracellular loop. Although an asparagine to serine substitution is considered a conservative substitution with respect to charge, NetPhos3.1 predicts that introducing a serine at *CLDN16* p.N223 creates a putative phosphorylation site. A glutamic acid to lysine switch results in a change

from a positive to a negatively charged residue. Finally, two of the variants affect amino acids in the C-terminal cytoplasmic domain. The proline to leucine substitution in *CLDN8* p.P216L introduces a hydrophobic side chain, while the glutamic acid to glycine substitution in the *CLDN19* p.E209G variant results in loss of a negatively charged amino acid and is considered a non-conservative change. Given that the claudin cytoplasmic C-terminal domain interacts with adaptor proteins that bridge the tight junction to the actin cytoskeleton, these variants have the potential to disrupt protein-protein interactions that regulate morphogenetic movements and cell shape changes during neural tube closure. Both *CLDN19* variants were present in the heterozygous state in the patients' mothers (Supplementary Figure S1). Genomic DNA was not available for the parents of the NTD patients with the *CLDN8* p.P216L, *CLDN9* p.S3L, *CLDN16* p.N223S, *CLDN18* p.V88I, and *CLDN24* p.E161K variants.

CLDN3 p.A128T and *CLDN24* p.G94R were not present in either the gnomAD or the EVS databases. The novel p.A128T variant was found in three unrelated NTD patients. The father of one patient and the mother of another patient were heterozygous for this allele (Supplementary Figure S1). Parental DNA was not available for the third patient. The patient that inherited the *CLDN3* p.A128T variant from their father also had a rare heterozygous mutation in the PCP gene *CELSR1* p.G934R [MIM: 604532] that is predicted to be benign (Allache et al., 2012). Parental DNA was not available for genetic testing for the single NTD patient with the *CLDN24* p.G94R variant. Both of these variants localize to transmembrane domains. An alanine to threonine substitution results in reduced hydrophobicity and may affect the ability of the protein to insert into the membrane, but does not create a putative phosphorylation site in CLDN3. The substitution of a glycine to arginine in CLDN24 introduces a positively charged bulky side chain that may have structural consequences.

CLDN Variants Do Not Affect the Ability of the Protein to Localize to Tight Junction Strands

Claudins are able to localize to cell-cell contacts and induce the formation of tight junction strands when transfected in tight junction-free HEK293 cells (Milatz et al., 2015; Piontek et al., 2017). To determine if the *CLDN* variants identified in the NTD patients affected the ability of the CLDN protein to localize to the cell membrane, we transiently transfected HEK293 cells with expression vectors containing the wild-type or variant *CLDN* cDNA. The ability of the claudin to co-localize with ZO-1, a classic component of the tight junction cytoplasmic plaque (Stevenson et al., 1986, 1989), was assessed. Wild-type and variant CLDN3, CLDN8, CLDN16, and CLDN19 proteins were able to co-localize with ZO-1 at points of cell-cell contact between neighboring transfected HEK 293 claudin-expressing cells (Figure 3), suggesting that these amino acid substitutions do not impact the ability of variant CLDN to integrate into a tight junction strand. Although the CLDN18 V88I protein was localized to cell-cell contacts, it appeared to be less tightly associated with the membrane than wild-type CLDN18.



Wild-type CLDN9 and 24 protein and their corresponding variants did not localize to the membrane in transiently transfected HEK293 cells (data not shown). To determine if

these claudins might require the presence of other claudin family members, we transiently transfected CLDN9 and CLDN24 cDNA expression vectors into MDCK II cells that express many claudin

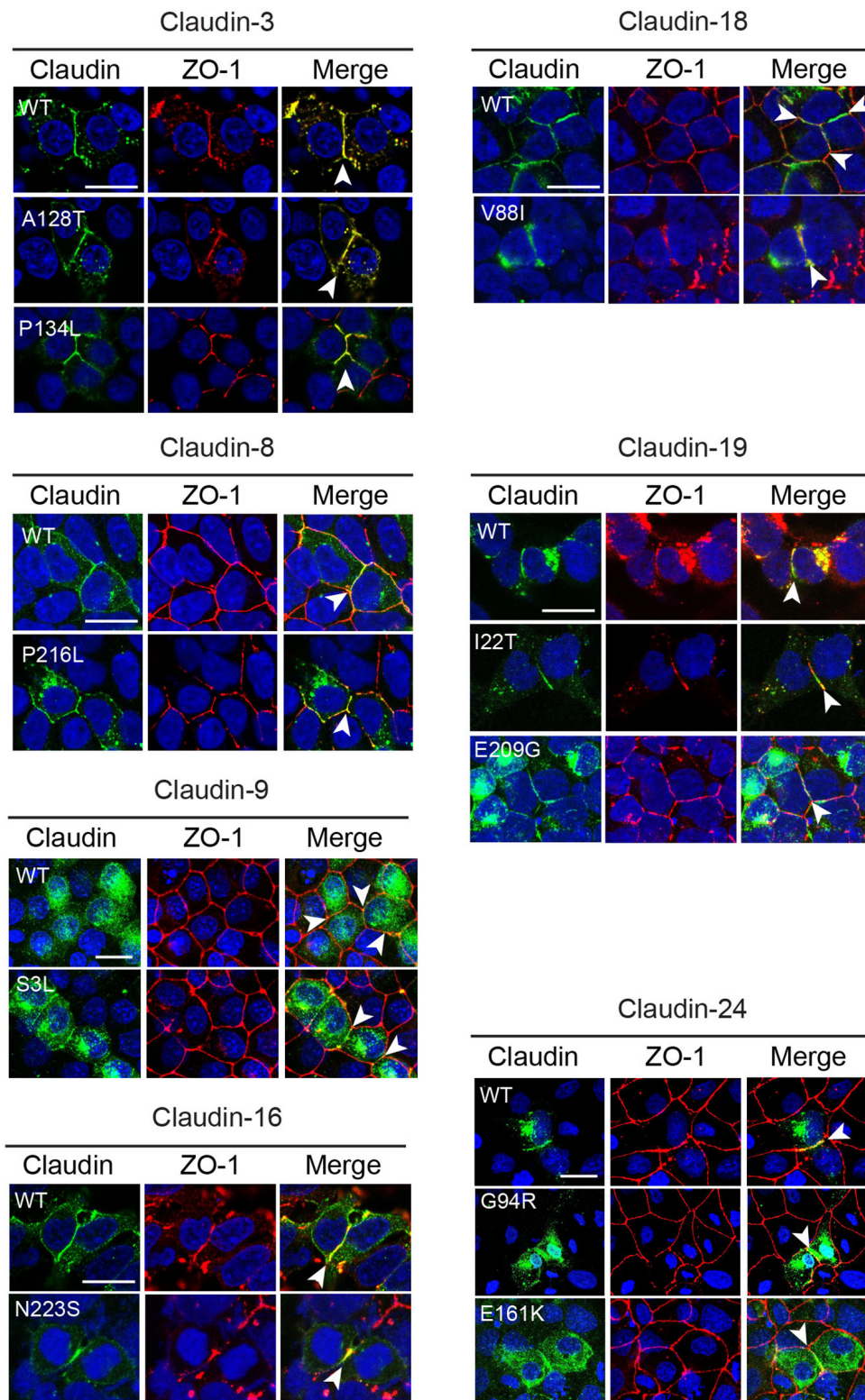


FIGURE 3 | Subcellular localization of CLDN variants. Wild-type (WT) and variant claudins (green) co-localized with the tight junction adaptor protein ZO-1 (red) at the cell membrane (arrowhead) in transiently transfected HEK293 (CLDN3, 4, 8, 16, 18, and 19) or MDCK II cells (Cldn9 and 24). Cldn3, -8, and -16 were detected with anti-claudin antibodies. Cldn9, -18, -19, and -24 were detected with an anti-HA antibody. Blue indicates DAPI stain of the nucleus. The images shown are maximum intensity projections. Scale bar, 20 μm .

family members and which are localized in tight junctions. In MDCK II cells, both wild-type CLDN9 and 24 protein co-localized with ZO-1 at cell contacts. The CLDN9 S3L and CLDN24 G94R and E161K variants did not affect the ability of the protein to localize to the tight junction (Figure 3). CLDN24 E161K was not subjected to further functional analyses because we were unable to confirm by Sanger sequencing due to lack of patient DNA.

These data support that the missense variants were able to co-localize with tight junction proteins similarly to the wild-type protein. Cytoplasmic accumulation of claudin proteins was observed for both wild-type and variant forms of each family member. This is likely to be a consequence of overexpression and not related to the variant.

Overexpressing CLDN3, CLDN8, and CLDN19 Variants Cause Open NTDs in Chick Embryos

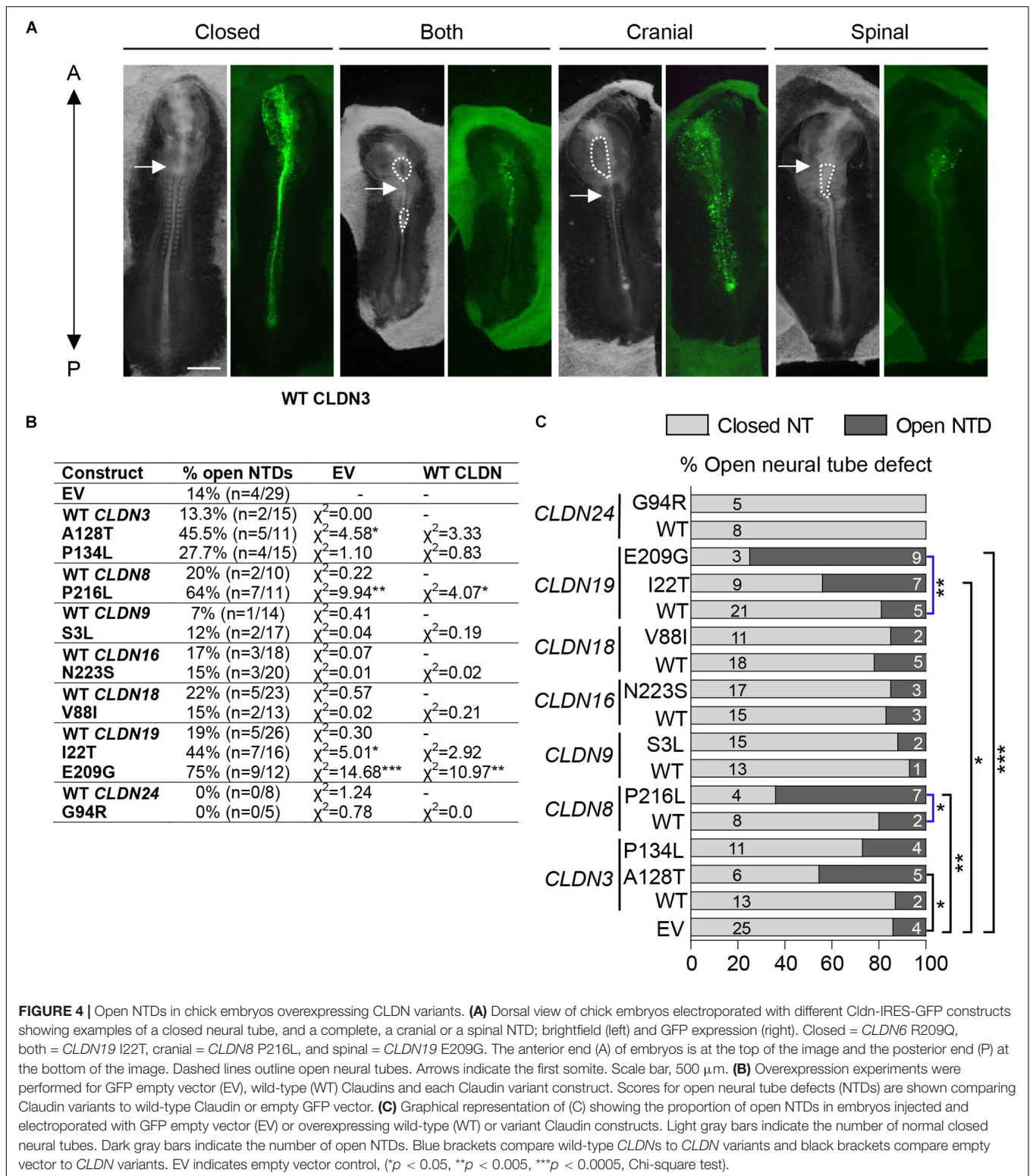
To investigate the potential pathogenic role of the rare and novel missense CLDN variants identified in NTD patients, we used an overexpression assay in the chick embryo model to examine the effect of these variants on neural tube closure. Previous studies have shown that knockdown or overexpression of NTD-related genes can lead to similar NTD phenotypes (Ting et al., 2003; Yu et al., 2006; Gustavsson et al., 2007; De Castro et al., 2018). The chick embryo is an excellent model to study neural tube closure for several reasons: (1) the tissue and cellular behaviors that regulate neurulation in the chick have been well-studied, (2) the morphogenetic movements regulating neural tube closure in chick and human embryos are predicted to be very similar, (3) neural tube closure occurs over a short period of time (~28 h) making it easy to collect a large number of embryos (Schoenwolf and Franks, 1984; Smith and Schoenwolf, 1987; Schoenwolf et al., 1988; Schoenwolf and Alvarez, 1989; Schoenwolf, 1991; Smith et al., 1994; Moury and Schoenwolf, 1995; Sausedo et al., 1997; Lawson et al., 2001; Kinoshita et al., 2008; Nishimura et al., 2012; Chen et al., 2017), and (4) the neural tube is easily accessible for manipulation in *ex ovo* culture.

Neural plate stage chick embryos (HH4) were injected and electroporated with GFP expression vectors encoding wild-type or variant human CLDNs and cultured *ex ovo* until they reached HH11-13, when they could be assessed for NTDs. A range of NTD phenotypes was observed varying from an opening in the future brain (cranial), an opening in the future spinal cord (spinal) or openings in the future brain and spinal cord (both) (Figure 4A). Our background level of NTDs due to experimental manipulation was 14% ($n = 4/29$) as determined by the electroporation of an 'empty' expression vector that expressed only GFP. Overexpression of wild-type CLDNs did not significantly affect neural tube closure as compared to control injected and electroporated embryos ($p > 0.05$, Figures 4B,C) suggesting that increased expression of wild-type CLDNs do not disrupt normal morphogenesis of the neural tube. Although predicted to be deleterious by *in silico* analysis, overexpression of CLDN3 P134L, CLDN9 S3L, CLDN16 N223S, CLDN18 V88I, and CLDN24 G94R did not increase the incidence of NTDs as

compared to wild-type CLDN3 ($\chi^2 = 0.83$, $p = 0.361$), CLDN9 ($\chi^2 = 0.19$, $p = 0.665$), CLDN16 ($\chi^2 = 0.02$, $p = 0.888$), CLDN18 ($\chi^2 = 0.81$, $p = 0.389$) and CLDN24 ($\chi^2 = 0.0$, $p = 0.0$) or control embryos (Figures 4B,C). In contrast, overexpression of CLDN3 A128T caused a significant increase in open NTDs compared to empty vector control embryos ($\chi^2 = 4.58$, $p = 0.0323$) and three times as many NTDs compared to wild-type CLDN3 ($\chi^2 = 3.33$, $p = 0.0681$) (Figures 4B,C). CLDN8 P216L also caused a significant increase in open NTDs compared to controls ($\chi^2 = 9.94$, $p = 0.00162$) and wild-type CLDN8 ($\chi^2 = 4.07$, $p = 0.0436$) (Figures 4B,C). Overexpression of CLDN19 I22T caused a significant increase in NTDs compared to empty vector control embryos ($\chi^2 = 5.01$, $p = 0.025$) and a twofold increase in the incidence of NTDs compared to wild-type CLDN19 ($\chi^2 = 2.92$, $p = 0.088$) (Figures 4B,C). Finally, a significant increase in open NTDs was observed in embryos electroporated with CLDN19 E209G compared to both wild-type CLDN19 ($\chi^2 = 10.97$, $p = 0.000924$) and empty vector control embryos ($\chi^2 = 14.68$, $p = 0.000127$) (Figures 4B,C).

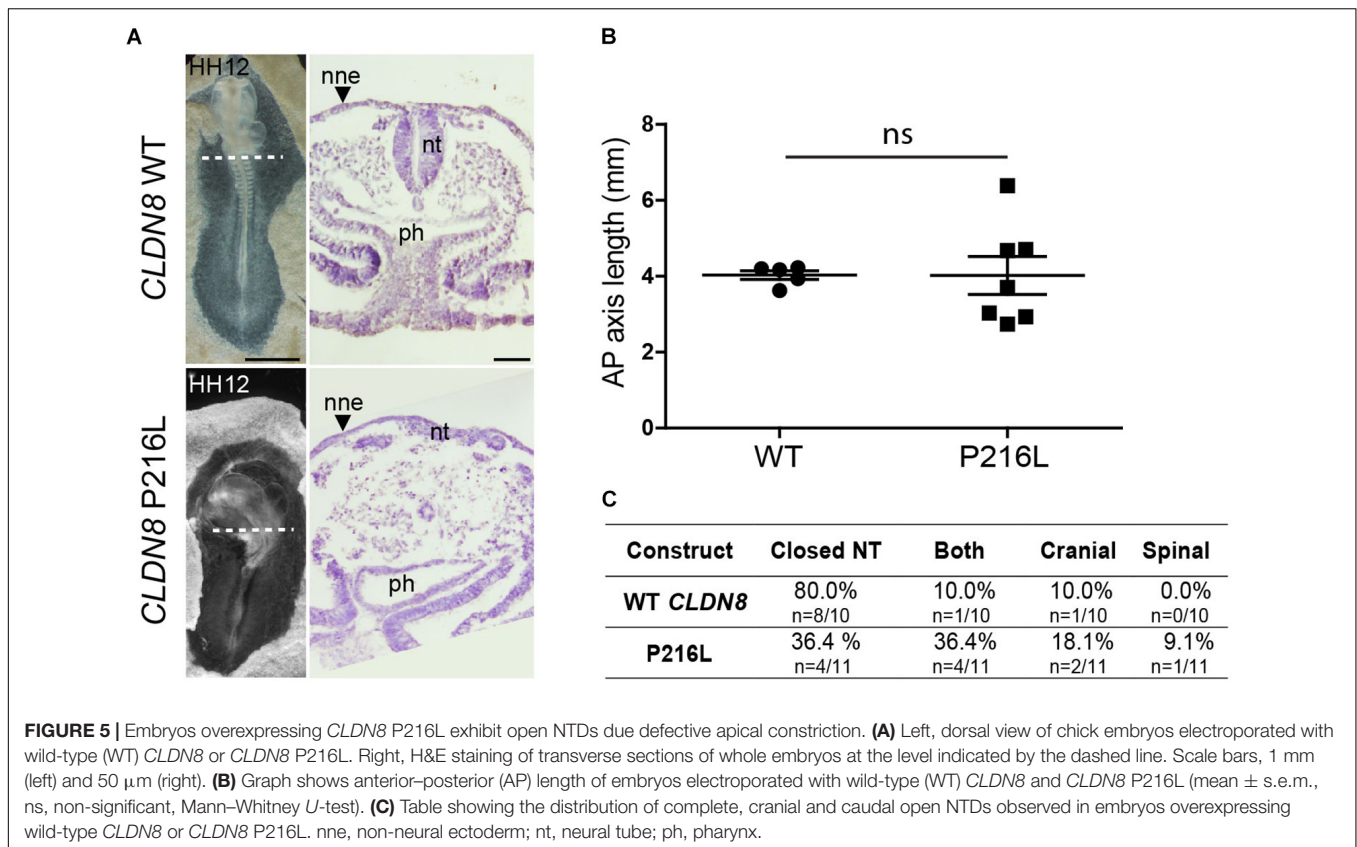
To identify the specific events of neural tube morphogenesis affected by overexpressing the CLDN variants, we investigated their effects on convergent extension and apical constriction. Convergent extension defects are manifested by a shortened and wider body axis, while a broadened neural tube midline is characteristic of defective apical constriction. Histological analysis of embryos overexpressing CLDN8 P216L revealed that the midline of the neural tube was flat and the neural folds failed to elevate at the level of open NTDs (Figure 5A). These data suggest that this variant impedes apical constriction of midline cells, which is essential for formation of the median hinge point and consequently elevation of the neural folds. However, they were of normal length compared to wild-type CLDN8 overexpressing embryos ($p = 0.8763$), indicating that convergent extension was not affected (Figure 5B). Finally, both cranial and spinal open NTDs were observed in these embryos (Figure 5C). In contrast, the NTDs observed in embryos overexpressing CLDN19 E209G appear to be due to defects in convergent extension. These embryos were significantly shorter than embryos overexpressing wild-type CLDN19 ($p = 0.0015$), but apical constriction to form the median hinge point appears to have occurred normally as evidenced by the wedge-shaped *Shh* expression domain at the neural tube midline (Greene et al., 1998; Ybot-Gonzalez et al., 2007) (Figures 6A,B). Overexpression of CLDN19 E209G generated a significant increase in spinal ($p = 0.0019$) and both cranial and spinal NTDs ($p = 0.0079$) compared to wild-type CLDN19 (Figure 6C).

In contrast to the severe NTDs observed when convergent extension or apical constriction events are impacted, the NTDs observed in embryos overexpressing CLDN19 I22T and CLDN3 A128T were relatively mild, with small openings along the entire length of the neural tube, suggestive of defects in neural fold fusion (Figures 6A, 7A). Although the CLDN3 A128T embryos were somewhat longer than embryos electroporated with wild-type CLDN3 ($p = 0.0007$), they were not longer than those overexpressing CLDN3 P134L ($p = 0.1023$), which did not cause a significant increase in the incidence of NTDs (Figures 4B, 7B). Overexpression of CLDN3 A128T caused a significant increase



in both cranial and spinal NTDs ($p = 0.0204$) compared to wild-type *CLDN3* (Figure 7C). Similarly, *CLDN19* I22T embryos did not exhibit apical constriction nor convergent extension defects. A cross section through the neural tube of these embryos revealed

that the neural folds elevated but failed to fuse suggesting that the NTDs are caused by defective fusion of the neural folds (Figure 6A). Together, these data indicate that the novel p.A128T variant in *CLDN3* and the rare variants p.P216L in *CLDN8*



and p.I22T and p.E209G in *CLDN19* identified in our NTD cohort are pathogenic.

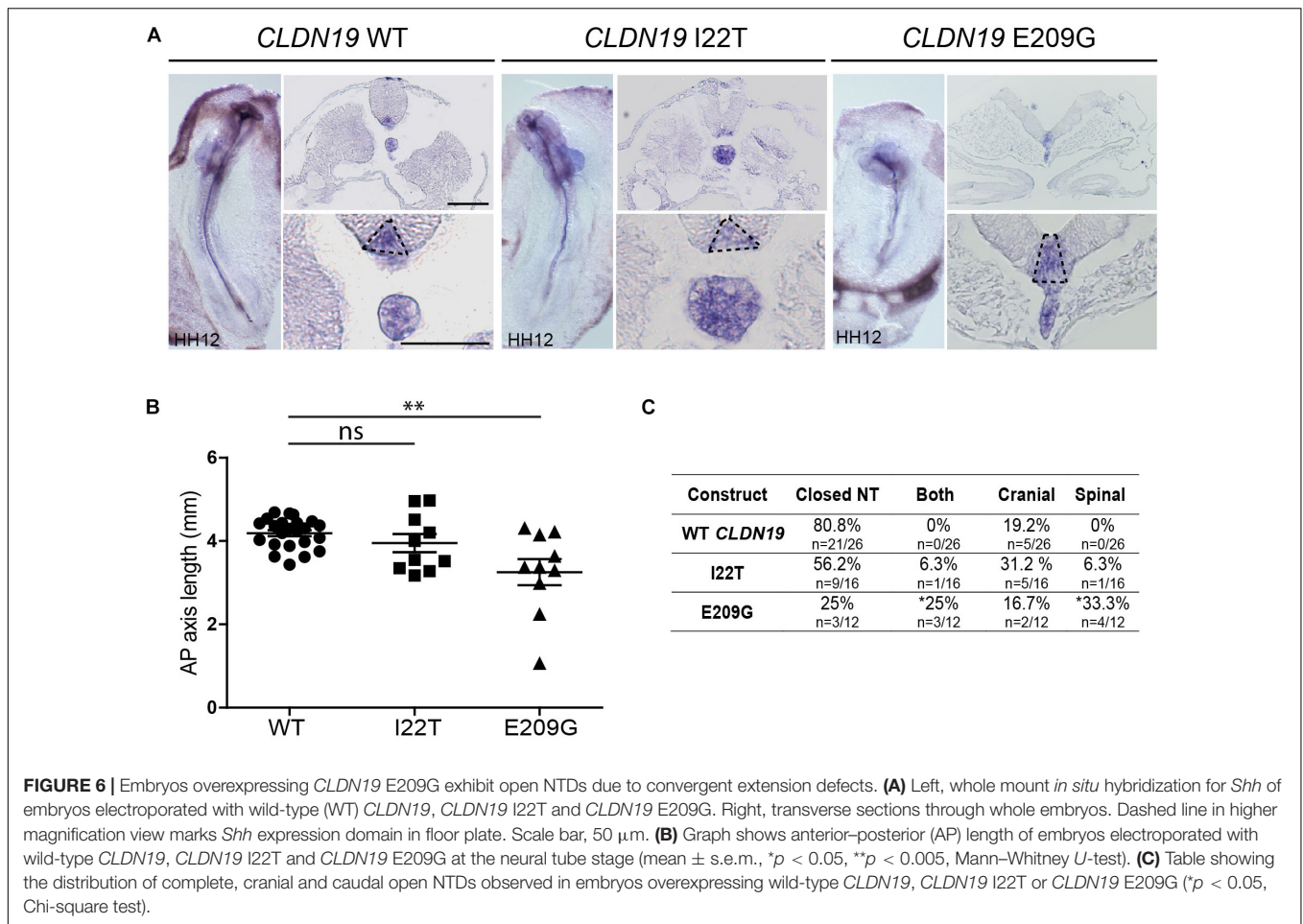
DISCUSSION

Previously we showed that depletion of *Cldn3*, -4, and -8 from tight junctions in the neural (*Cldn4* and -8) and non-neural ectoderm (*Cldn3* and -4) results in NTDs in chick and mouse embryos (Baumholtz et al., 2017). Morphological analysis of chick embryos revealed that these claudins play critical roles in regulating convergent extension and apical constriction, two morphogenetic events that drive neural tube closure (Baumholtz et al., 2017). However, the possible contribution of rare and novel mutations in *CLDN* genes to human NTDs has not yet been studied. Using a targeted high-throughput sequencing strategy for *CLDN* genes, we identified 17 common, 11 rare and four novel variants in a cohort of 152 NTD patients with the open spinal NTD myelomeningocele. Eight of the rare variants (*CLDN3* p.P134L, *CLDN8* p.P216L, *CLDN9* p.S3L, *CLDN16* p.N223S, *CLDN18* p.V88I, *CLDN19* p.I22T and p.E209G, and *CLDN24* p.E161K) and two of the novel *CLDN* variants (*CLDN3* p.A128T and *CLDN24* p.G94R) were predicted to be pathogenic by at least one prediction program. Overexpression assays in a chick embryo model demonstrated that *CLDN3* A128T, *CLDN8* P216L, and *CLDN19* I22T and E209G generated a significant increase in open NTDs compared to overexpression of the 'empty' vector or the

wild-type *CLDN*. All of these variants appear to localize normally to tight junctions at cell-cell contacts, which suggests that they may contribute to NTDs by interfering with protein-protein interactions at the tight junction. Our data suggest that variants in *CLDN* proteins may underlie a subset of human NTDs.

Pathogenic *CLDN* variants could affect neural tube closure by three possible mechanisms. First, they may function as null alleles due to effects on protein stability, function or tight junction localization and cause NTDs due to insufficient levels of the claudin protein at the tight junction. Second, the variant may lead to the production of a dominant negative protein that could compete with wild-type protein for incorporation into tight junction strands, but once there it would impede the function of wild-type claudins. Finally, the variant may predispose an individual to having an NTD but be insufficient to independently cause an NTD. In these cases, we would predict that a 'second hit' such as a variant in another claudin family member or a component of an intersecting pathway would be required to induce NTDs.

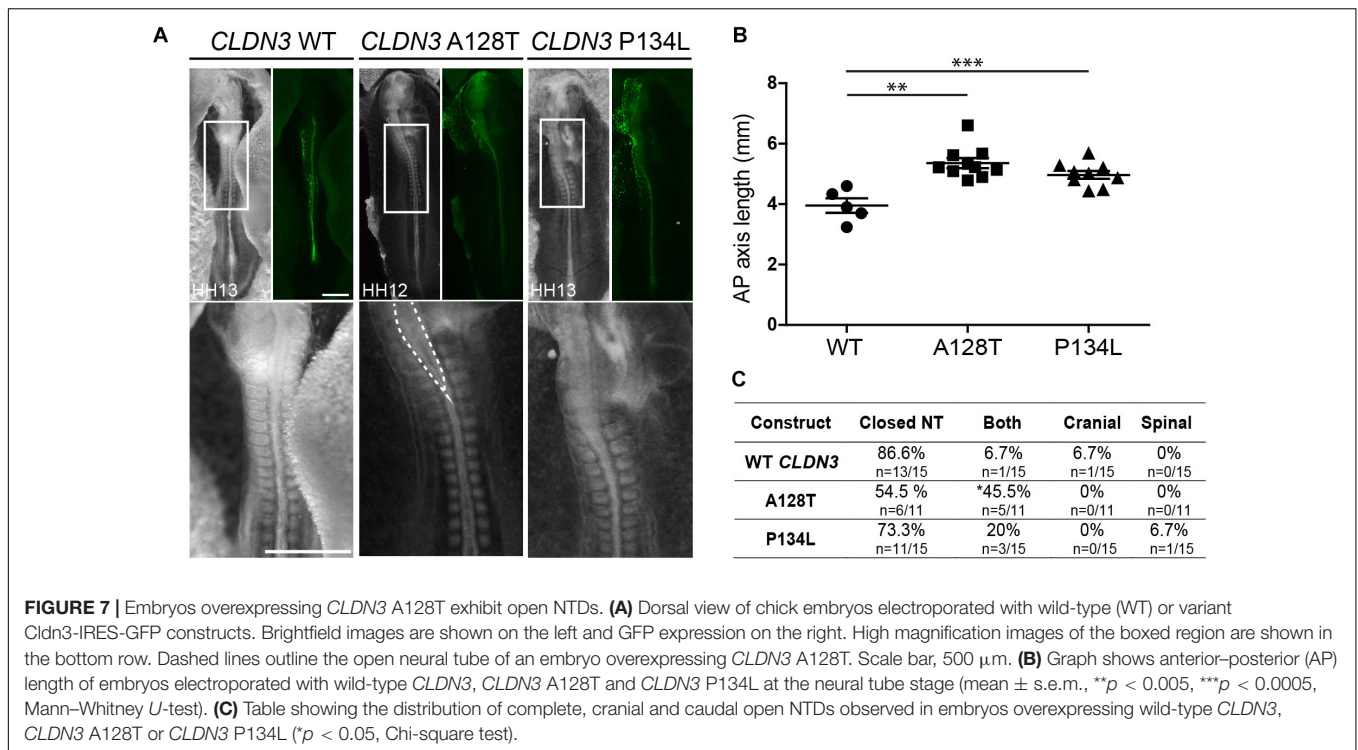
None of the *CLDN* variants that we identified in this myelomeningocele cohort were truncating alleles nor predicted to generate a null allele. Moreover, we did not expect a claudin null allele to cause an NTD given that none of the *CLDN* null mice have NTDs (Gow et al., 1999; Furuse et al., 2002; Ben-Yosef et al., 2003; Nitta et al., 2003; Kitajiri et al., 2004; Anderson et al., 2008; Tamura et al., 2008; Nakano et al., 2009; Muto et al., 2010; Ding et al., 2012; Fujita et al., 2012; Hayashi et al., 2012;



Kage et al., 2014; Kooij et al., 2014; Li et al., 2014; Matsumoto et al., 2014; Ahmad et al., 2017; Bardet et al., 2017). Although a *Cldn8* null mouse has not yet been reported, *Cldn3* (Kooij et al., 2014; Ahmad et al., 2017; Bardet et al., 2017) and *Cldn19* null mice (Miyamoto et al., 2005) have closed neural tubes. This is perhaps not surprising as knockout or knockdown of a single claudin often results in compensatory upregulation of another family member (Li et al., 2014). Indeed previous data from our lab showed that depleting *Cldn4* led to an increase in the level of *Cldn8* in the neural ectoderm that is predicted to be compensatory, as the *Cldn4*-depleted chick embryos developed normally (Baumholtz et al., 2017). In addition, all were able to co-localize with ZO-1 at tight junctions in transfected cells as effectively as the wild-type claudin, suggesting that they do not impede the ability of the claudin protein to localize to tight junctions. However, it is possible that these variant alleles affect the tight junction barrier and future studies are needed to address this question.

Our overexpression functional assay in chick embryos is most effective at identifying variants that have the potential to act as ‘dominant negatives’ or ‘competitive inhibitors’ since we are expressing them in the context of a full complement of wild-type claudins. We noted that overexpression of wild-type

CLDNs did not cause NTDs suggesting that higher levels of a wild-type claudin protein are not pathogenic. We tested the functional pathogenicity of nine variants that were predicted to be pathogenic by one or more analysis software programs. Four of these variants caused open NTDs when overexpressed in chick embryos, while overexpression of the corresponding wild-type *CLDN* did not. Interestingly, the distinct phenotypes observed when pathogenic variants were overexpressed in chick embryos correlate with the position of the variant in the claudin protein and suggest that claudins function in multiple phases of neural tube closure. *CLDN19* I22T and *CLDN3* A128T, which are in the first and third transmembrane domains, respectively, caused a significant increase in NTDs in chick embryos due to defects in the fusion of the neural folds to form a closed neural tube. Both variants change the amino acid in the transmembrane domain to a threonine, which has the potential to disrupt heteromeric *cis*-interactions between claudins and the morphology of tight junction strands (Rossa et al., 2014). In addition, *CLDN19* p.I22T, but not *CLDN3* p.A128T, introduces a putative phosphorylation site that could induce a further conformational change. These alterations to tight junction morphology could affect tight junction barrier properties.



The mechanism by which *CLDN3* and *CLDN19* could regulate neural fold fusion remains unknown, but may relate to their function in regulating the tight junction barrier. In addition, *Cldn3* expression is limited to the non-neural ectoderm (Simard et al., 2006; Baumholtz et al., 2017), which functions primarily in neural fold fusion. The initial contact between apposing neural folds is mediated by extracellular matrix proteins secreted from the neural and non-neural ectoderm in the chick embryo. It was shown that *Cldn3* and -19 are located in tight junctions of ameloblasts in the mouse tooth germ where they play a role in regulating extracellular pH, which is critical for processing and secretion of extracellular matrix proteins (Bardet et al., 2017; Yamaguti et al., 2017). *Cldn3* knockout mice exhibit enamel defects caused by excess accumulation of extracellular matrix proteins in the forming enamel and mutations in *CLDN19* are associated with Amelogenesis Imperfecta, a genetic disorder characterized by tooth enamel defects (Bardet et al., 2017; Yamaguti et al., 2017). The *CLDN3* p.A128T and *CLDN19* p.I22T mutations located in the transmembrane domains of these barrier and pore-forming claudins, respectively, could affect the tight junction barrier leading to a pH imbalance in the extracellular space and lack of secretion of extracellular matrix proteins that are critical for mediating the initial contact between apposed neural folds. The hypothesis will be explored in future studies to understand the mechanisms by which these claudins affect the tight junction barrier.

More dramatic open NTDs due to failures in apical constriction and convergent extension were caused by pathogenic variants in the cytoplasmic C-terminal domain, *CLDN8* P216L and *CLDN19* E209G, respectively. The NTDs in the *CLDN8*

P216L and *CLDN19* E209G embryos closely resembled those observed in the embryos that were depleted for *Cldn3*, 4 and 8. Apical constriction and convergent extension are both early steps in neural tube morphogenesis that depend on cell-shape remodeling and cell–cell interactions. The claudin C-terminal cytoplasmic domain interacts directly with proteins in the tight junction cytoplasmic plaque, which interacts with the actin-cytoskeleton and is a docking site for several regulatory proteins. The *CLDN8* p.P216L variant is likely to alter the conformation of the cytoplasmic C-terminal tail, while the *CLDN19* p.E209G variant results in loss of a negatively charged amino acid immediately adjacent to the cytoplasmic C-terminal PDZ-binding domain. Both of these variants have the potential to disrupt interactions with the cytoplasmic tail, including PDZ-domain adaptor proteins that connect the tight junction to the actin cytoskeleton. In particular, the loss of a negatively charged amino acid is predicted to destabilize interactions with partners that play critical roles in neural tube morphogenesis.

The myelomeningocele patient in our study cohort with the *CLDN8* p.P216L variant was of African ancestry. Given that the MAF is >3% in both African Americans in the EVS database and Africans in the gnomAD database, we would predict that this variant alone is not sufficient to cause NTDs in humans. However, we cannot rule out that it is a risk factor and could predispose the embryo to develop an NTD in the context of a second genetic hit or an environmental insult.

One limitation to our functional validation assay in the chick embryos is our inability to test whether the remaining 5 pathogenic variants generate hypomorphic alleles that may confer significant risk for NTDs in the context of a second

mutation or environmental insult. Components of the PCP pathway have a well-established role in regulating convergent extension movements during neural tube closure (Greene et al., 1998; Goto and Keller, 2002; Wallingford and Harland, 2002; Curtin et al., 2003; Wang J. et al., 2006; Wang Y. et al., 2006; Ybot-Gonzalez et al., 2007; Paudyal et al., 2010) and mutations in PCP pathway genes have been recognized as risk factors for human NTDs (Kibar et al., 2009, 2011; Lei et al., 2010; Bosoi et al., 2011; Allache et al., 2012; De Marco et al., 2012, 2013; Robinson et al., 2012). We previously showed that claudins act upstream of PCP signaling and convergent extension during neural tube closure (Baumholtz et al., 2017). Interestingly, four patients with a rare or novel mutation in a *CLDN* gene also carried a PCP gene variant. Only one of these four *CLDN* variants caused NTDs in our overexpression assay (*CLDN3* p. A128T) in the chick embryo. However, it is possible that all four act synergistically with the PCP variants, thereby conferring a high risk for NTDs – a two-hit model for NTDs. This digenic model for NTDs has been observed in mice carrying mutations in PCP genes where homozygous mice have a closed neural tube (e.g., *Fzd3*^{-/-} or *Fzd6*^{-/-}) (Wang et al., 2002; Guo et al., 2004), while double homozygous mice (e.g., *Fzd3*^{-/-};*Fzd6*^{-/-}) develop NTDs (Wang Y. et al., 2006). Furthermore, heterozygous mice with spinal NTDs (e.g., *Vangl2*^{Lp/+}) develop craniorachischisis, a severe NTD that affects the entire embryonic axis, when crossed to heterozygous mice carrying a mutations in a second PCP gene (e.g., *Vangl2*^{Lp/+}; *Scrib*^{Crc/+}, *Vangl2*^{Lp/+}; *Celsr1*^{Crsh/+}, *Vangl2*^{Lp/+}; *Ptk7*^{chz/+}) (Murdoch et al., 2014). It would be interesting to determine if there are genetic interactions between the *CLDN* and *PCP* variants detected in the same patient. In addition, the remaining patients should be screened for mutations in PCP genes.

The mechanisms involved in spinal NTDs are thought to differ from those of cranial NTDs; apical constriction is more important for cranial neural tube closure, while convergent extension plays a more critical role in spinal neural tube closure in chick embryos. Fusion of the neural folds to form a closed neural tube occurs at the cranial and spinal levels. We have shown that claudins are required for apical constriction and convergent extension and thus, mutations in *CLDN* genes may be implicated in both cranial and spinal NTDs. In the future, it would be interesting to sequence genomic DNA from patients with cranial NTDs to compare the pathogenesis of rare and novel *CLDN* variants in the different types of NTDs.

CONCLUSION

Our study highlights the conserved function of claudins among species in neural tube closure and supports the hypothesis that rare deleterious variants in *CLDN* genes are significant risk factors for human spinal NTDs. Furthermore, our study demonstrates the importance of validating pathogenicity in a biological system rather than strictly relying on predictive programs: while *CLDN3* p.P134L, *CLDN9* p.S3L, *CLDN18* p.V88I, and *CLDN24* p.G94R were predicted to be pathogenic by all three prediction program, they did not affect the

ability of the Cldn protein to localize to tight junctions or cause NTDs in our overexpression assay. In contrast, the *CLDN8* p.P216L variant was predicted to be benign SIFT and MutationTaster, yet overexpression of this variant caused a significant increase in NTDs in our overexpression assay. This highlights the limitation of relying on *in silico* prediction programs to predict pathogenicity of non-synonymous variants which exploit limited information such as amino evolutionary conservation and properties, and do not consider known protein functional domains or tissue-specific protein functions. To our knowledge, this is the first study to identify deleterious variants in *CLDN* genes in patients with NTDs, which further supports the concept that human NTDs are a group of disorders with high genetic heterogeneity, and both *CLDN* and PCP genomic variants contribute to their occurrence. These results enhance our understanding of the pathogenesis of NTDs in humans, highlighting the importance of considering variants in the claudin family as new candidates for NTDs in humans.

DATA AVAILABILITY STATEMENT

The datasets for this article are not publicly available because of ethical and legal reasons. Requests to access the datasets should be directed to VC at valeriacapra@gaslini.org.

ETHICS STATEMENT

The studies involving human participants were reviewed and approved by IRCCS Istituto Giannina Gaslini (Protocol number: IGG-VACA, 18 September 2011) Research Institute of the McGill University Health Centre (Protocol number: 14-444-PED). Written informed consent to participate in this study was provided by the participants' legal guardian/next of kin.

AUTHOR CONTRIBUTIONS

AB and AR conceptualized the study. AR supervised the implementation and helped with data analysis and drafting the manuscript. AB conducted the cell and chick functional experiments, performed the bioinformatic data analysis, and participated in drafting the manuscript. VC provided critical comments of the manuscript and participated in subject enrollment. PD participated in subject enrollment and extracted genomic DNA from the blood of enrolled patients. All authors contributed to the article and approved the submitted version.

FUNDING

This work was supported by the Natural Sciences and Engineering Research Council of Canada (grant number 234319 to AR), a pilot project grant from the Montreal Children's Hospital Foundation (to AR) and ASBI, association for Italian

parents supports (to VC). AR is a member of the RI-MUHC, which was supported in part by the FRQ-S. AB is the recipient of a doctoral fellowship from the Fonds Recherché du Québec – Santé (FRQS, 29939).

ACKNOWLEDGMENTS

We thank the families for their participation. We would also like to thank C. Goodyer, I. Gupta, L. Jerome-Majewska, P. Siegel,

and Y. Yamanaka for helpful discussions, and M. Fu (RI-MUHC Imaging Platform) and P. Lepage (Genome Quebec) for technical assistance.

SUPPLEMENTARY MATERIAL

The Supplementary Material for this article can be found online at: <https://www.frontiersin.org/articles/10.3389/fnins.2020.00664/full#supplementary-material>

REFERENCES

- Adzhubei, I. A., Schmidt, S., Peshkin, L., Ramensky, V. E., Gerasimova, A., Bork, P., et al. (2010). A method and server for predicting damaging missense mutations. *Nat. Methods* 7, 248–249. doi: 10.1038/nmeth0410-248
- Ahmad, R., Kumar, B., Chen, Z., Chen, X., Muller, D., Lele, S. M., et al. (2017). Loss of claudin-3 expression induces IL6/gp130/Stat3 signaling to promote colon cancer malignancy by hyperactivating Wnt/beta-catenin signaling. *Oncogene* 36, 6592–6604. doi: 10.1038/onc.2017.259
- Allache, R., De Marco, P., Merello, E., Capra, V., and Kibar, Z. (2012). Role of the planar cell polarity gene CELSR1 in neural tube defects and caudal agenesis. *Birth Defects Res. A Clin. Mol. Teratol.* 94, 176–181. doi: 10.1002/bdra.23002
- Anderson, W. J., Zhou, Q., Alcalde, V., Kaneko, O. F., Blank, L. J., Sherwood, R. I., et al. (2008). Genetic targeting of the endoderm with claudin-6CreER. *Dev. Dyn.* 237, 504–512. doi: 10.1002/dvdy.21437
- Bardet, C., Ribes, S., Wu, Y., Diallo, M. T., Salmon, B., Breiderhoff, T., et al. (2017). Claudin loss-of-function disrupts tight junctions and impairs amelogenesis. *Front. Physiol.* 8:326. doi: 10.3389/fphys.2017.00326
- Baumholtz, A. I., Simard, A., Nikolopoulou, E., Oosenbrug, M., Collins, M. M., Piontek, A., et al. (2017). Claudins are essential for cell shape changes and convergent extension movements during neural tube closure. *Dev. Biol.* 428, 25–38. doi: 10.1016/j.ydbio.2017.05.013
- Ben-Yosef, T., Belyantseva, I. A., Saunders, T. L., Hughes, E. D., Kawamoto, K., Van Itallie, C. M., et al. (2003). Claudin 14 knockout mice, a model for autosomal recessive deafness DFNB29, are deaf due to cochlear hair cell degeneration. *Hum. Mol. Genet.* 12, 2049–2061. doi: 10.1093/hmg/ddg210
- Blom, N., Gammeltoft, S., and Brunak, S. (1999). Sequence and structure-based prediction of eukaryotic protein phosphorylation sites. *J. Mol. Biol.* 294, 1351–1362. doi: 10.1006/jmbi.1999.3310
- Bosoi, C. M., Capra, V., Allache, R., Trinh, V. Q., De Marco, P., Merello, E., et al. (2011). Identification and characterization of novel rare mutations in the planar cell polarity gene PRICKLE1 in human neural tube defects. *Hum. Mutat.* 32, 1371–1375. doi: 10.1002/humu.21589
- Bruel, A. L., Franco, B., Duffourd, Y., Thevenon, J., Jego, L., Lopez, E., et al. (2017). Fifteen years of research on oral-facial-digital syndromes: from 1 to 16 causal genes. *J. Med. Genet.* 54, 371–380. doi: 10.1136/jmedgenet-2016-104436
- Chen, G., Pei, L. J., Huang, J., Song, X. M., Lin, L. M., Gu, X., et al. (2009). Unusual patterns of neural tube defects in a high risk region of northern China. *Biomed. Environ. Sci.* 22, 340–344. doi: 10.1016/s0895-3988(09)60065-9
- Chen, X., An, Y., Gao, Y., Guo, L., Rui, L., Xie, H., et al. (2017). Rare Deleterious PARD3 Variants in the aPKC-binding region are implicated in the pathogenesis of human cranial neural tube defects via disrupting apical tight junction formation. *Hum. Mutat.* 38, 378–389. doi: 10.1002/humu.23153
- Collins, M. M., and Ryan, A. K. (2011). Manipulating claudin expression in avian embryos. *Methods Mol. Biol.* 762, 195–212. doi: 10.1007/978-1-61779-185-7_14
- Curtin, J. A., Quint, E., Tspouri, V., Arkell, R. M., Cattanach, B., Copp, A. J., et al. (2003). Mutation of Celsr1 disrupts planar polarity of inner ear hair cells and causes severe neural tube defects in the mouse. *Curr. Biol.* 13, 1129–1133. doi: 10.1016/s0960-9822(03)00374-9
- De Castro, S. C. P., Gustavsson, P., Marshall, A. R., Gordon, W. M., Galea, G., Nikolopoulou, E., et al. (2018). Overexpression of Grainyhead-like 3 causes spina bifida and interacts genetically with mutant alleles of Grhl2 and Vangl2 in mice. *Hum. Mol. Genet.* 27, 4218–4230. doi: 10.1093/hmg/ddy313
- De Marco, P., Merello, E., Consales, A., Piatelli, G., Cama, A., Kibar, Z., et al. (2013). Genetic analysis of disheveled 2 and disheveled 3 in human neural tube defects. *J. Mol. Neurosci.* 49, 582–588. doi: 10.1007/s12031-012-9871-9
- De Marco, P., Merello, E., Rossi, A., Piatelli, G., Cama, A., Kibar, Z., et al. (2012). FZD6 is a novel gene for human neural tube defects. *Hum. Mutat.* 33, 384–390. doi: 10.1002/humu.21643
- Ding, L., Lu, Z., Foreman, O., Tatum, R., Lu, Q., Renegar, R., et al. (2012). Inflammation and disruption of the mucosal architecture in claudin-7-deficient mice. *Gastroenterology* 142, 305–315. doi: 10.1053/j.gastro.2011.10.025
- Escuin, S., Vernay, B., Savery, D., Gurniak, C. B., Witke, W., Greene, N. D., et al. (2015). Rho-kinase-dependent actin turnover and actomyosin disassembly are necessary for mouse spinal neural tube closure. *J. Cell Sci.* 128, 2468–2481. doi: 10.1242/jcs.164574
- Exome Variant Server (2020). *NHLBI GO Exome Sequencing Project (ESP)*. Available at: <http://evs.gs.washington.edu/EVS/> (accessed 04, 2020).
- Fredriksson, K., Van Itallie, C. M., Aponte, A., Gucek, M., Tietgens, A. J., and Anderson, J. M. (2015). Proteomic analysis of proteins surrounding occludin and claudin-4 reveals their proximity to signaling and trafficking networks. *PLoS One* 10:e0117074. doi: 10.1371/journal.pone.0117074
- Fujita, H., Hamazaki, Y., Noda, Y., Oshima, M., and Minato, N. (2012). Claudin-4 deficiency results in urothelial hyperplasia and lethal hydronephrosis. *PLoS One* 7:e52272. doi: 10.1371/journal.pone.0052272
- Furuse, M., Hata, M., Furuse, K., Yoshida, Y., Haratake, A., Sugitani, Y., et al. (2002). Claudin-based tight junctions are crucial for the mammalian epidermal barrier: a lesson from claudin-1-deficient mice. *J. Cell Biol.* 156, 1099–1111. doi: 10.1083/jcb.200110122
- Goto, T., and Keller, R. (2002). The planar cell polarity gene strabismus regulates convergence and extension and neural fold closure in *Xenopus*. *Dev. Biol.* 247, 165–181. doi: 10.1006/dbio.2002.0673
- Gow, A., Southwood, C. M., Li, J. S., Pariali, M., Riordan, G. P., Brodie, S. E., et al. (1999). CNS myelin and sertoli cell tight junction strands are absent in *Osp/claudin-11* null mice. *Cell* 99, 649–659. doi: 10.1016/s0092-8674(00)81553-6
- Greene, N. D., Gerrelli, D., Van Straaten, H. W., and Copp, A. J. (1998). Abnormalities of floor plate, notochord and somite differentiation in the loop-tail (Lp) mouse: a model of severe neural tube defects. *Mech. Dev.* 73, 59–72. doi: 10.1016/s0925-4773(98)00029-x
- Guo, N., Hawkins, C., and Nathans, J. (2004). Frizzled6 controls hair patterning in mice. *Proc. Natl. Acad. Sci. U.S.A.* 101, 9277–9281. doi: 10.1073/pnas.0402802101
- Gustavsson, P., Greene, N. D., Lad, D., Pauws, E., de Castro, S. C., Stanier, P., et al. (2007). Increased expression of Grainyhead-like-3 rescues spina bifida in a folate-resistant mouse model. *Hum. Mol. Genet.* 16, 2640–2646. doi: 10.1093/hmg/ddm221
- Hamazaki, Y., Itoh, M., Sasaki, H., Furuse, M., and Tsukita, S. (2002). Multi-PDZ domain protein 1 (MUPP1) is concentrated at tight junctions through its possible interaction with claudin-1 and junctional adhesion molecule. *J. Biol. Chem.* 277, 455–461. doi: 10.1074/jbc.m109005200
- Hayashi, D., Tamura, A., Tanaka, H., Yamazaki, Y., Watanabe, S., Suzuki, K., et al. (2012). Deficiency of claudin-18 causes paracellular H⁺ leakage, up-regulation of interleukin-1beta, and atrophic gastritis in mice. *Gastroenterology* 142, 292–304. doi: 10.1053/j.gastro.2011.10.040
- Ikari, A., Matsumoto, S., Harada, H., Takagi, K., Hayashi, H., Suzuki, Y., et al. (2006). Phosphorylation of paracellin-1 at Ser217 by protein kinase A is

- essential for localization in tight junctions. *J. Cell Sci.* 119(Pt 9), 1781–1789. doi: 10.1242/jcs.02901
- Kage, H., Flodby, P., Gao, D., Kim, Y. H., Marconett, C. N., DeMaio, L., et al. (2014). Claudin 4 knockout mice: normal physiological phenotype with increased susceptibility to lung injury. *Am. J. Physiol. Lung Cell Mol. Physiol.* 307, L524–L536. doi: 10.1152/ajplung.00077.2014
- Karczewski, K. J., Francioli, L. C., Tiao, G., Cummings, B. B., Alfoldi, J., Wang, Q., et al. (2020). The mutational constraint spectrum quantified from variation in 141,456 humans. *bioRxiv [Preprint]* doi: 10.1101/531210
- Katahira, J., Inoue, N., Horiguchi, Y., Matsuda, M., and Sugimoto, N. (1997). Molecular cloning and functional characterization of the receptor for *Clostridium perfringens* enterotoxin. *J. Cell Biol.* 136, 1239–1247. doi: 10.1083/jcb.136.6.1239
- Kibar, Z., Bosoi, C. M., Kooistra, M., Salem, S., Finnell, R. H., De Marco, P., et al. (2009). Novel mutations in VANGL1 in neural tube defects. *Hum. Mutat.* 30, E706–E715.
- Kibar, Z., Salem, S., Bosoi, C. M., Pauwels, E., De Marco, P., Merello, E., et al. (2011). Contribution of VANGL2 mutations to isolated neural tube defects. *Clin. Genet.* 80, 76–82. doi: 10.1111/j.1399-0004.2010.01515.x
- Kinoshita, N., Sasai, N., Misaki, K., and Yonemura, S. (2008). Apical accumulation of Rho in the neural plate is important for neural plate cell shape change and neural tube formation. *Mol. Biol. Cell* 19, 2289–2299. doi: 10.1091/mbc.e07-12-1286
- Kitajiri, S., Miyamoto, T., Mineharu, A., Sonoda, N., Furuse, K., Hata, M., et al. (2004). Compartmentalization established by claudin-11-based tight junctions in stria vascularis is required for hearing through generation of endocochlear potential. *J. Cell Sci.* 117(Pt 21), 5087–5096. doi: 10.1242/jcs.01393
- Kooij, G., Kopplin, K., Blasig, R., Stuiver, M., Koning, N., Goverse, G., et al. (2014). Disturbed function of the blood-cerebrospinal fluid barrier aggravates neuro-inflammation. *Acta Neuropathol.* 128, 267–277. doi: 10.1007/s00401-013-1227-1
- Krause, G., Protze, J., and Piontek, J. (2015). Assembly and function of claudins: structure-function relationships based on homology models and crystal structures. *Semin. Cell Dev. Biol.* 42, 3–12. doi: 10.1016/j.semcdb.2015.04.010
- Lawson, A., Anderson, H., and Schoenwolf, G. C. (2001). Cellular mechanisms of neural fold formation and morphogenesis in the chick embryo. *Anat. Rec.* 262, 153–168. doi: 10.1002/1097-0185(20010201)262:2<153::aid-ar1021>3.0.co;2-w
- Lei, Y., Kim, S. E., Chen, Z., Cao, X., Zhu, H., Yang, W., et al. (2019). Variants identified in PTK7 associated with neural tube defects. *Mol. Genet. Genomic Med.* 7:e584. doi: 10.1002/mgg3.584
- Lei, Y. P., Zhang, T., Li, H., Wu, B. L., Jin, L., and Wang, H. Y. (2010). VANGL2 mutations in human cranial neural-tube defects. *N. Engl. J. Med.* 362, 2232–2235.
- Li, G., Flodby, P., Luo, J., Kage, H., Sipos, A., Gao, D., et al. (2014). Knockout mice reveal key roles for claudin 18 in alveolar barrier properties and fluid homeostasis. *Am. J. Respir. Cell Mol. Biol.* 51, 210–222. doi: 10.1165/rcmb.2013-0353OC
- Li, H., Zhang, J., Chen, S., Wang, F., Zhang, T., and Niswander, L. (2018). Genetic contribution of retinoid-related genes to neural tube defects. *Hum. Mutat.* 39, 550–562. doi: 10.1002/humu.23397
- Manolio, T. A., Collins, F. S., Cox, N. J., Goldstein, D. B., Hindorf, L. A., Hunter, D. J., et al. (2009). Finding the missing heritability of complex diseases. *Nature* 461, 747–753. doi: 10.1038/nature08494
- Matsumoto, K., Imasato, M., Yamazaki, Y., Tanaka, H., Watanabe, M., Eguchi, H., et al. (2014). Claudin 2 deficiency reduces bile flow and increases susceptibility to cholesterol gallstone disease in mice. *Gastroenterology* 147:1134–45.e10.
- Milatz, S., Piontek, J., Schulzke, J. D., Blasig, I. E., Fromm, M., and Gunzel, D. (2015). Probing the cis-arrangement of prototype tight junction proteins claudin-1 and claudin-3. *Biochem. J.* 468, 449–458. doi: 10.1042/bj20150148
- Miyamoto, T., Morita, K., Takemoto, D., Takeuchi, K., Kitano, Y., Miyakawa, T., et al. (2005). Tight junctions in Schwann cells of peripheral myelinated axons: a lesson from claudin-19-deficient mice. *J. Cell Biol.* 169, 527–538. doi: 10.1083/jcb.200501154
- Moury, J. D., and Schoenwolf, G. C. (1995). Cooperative model of epithelial shaping and bending during avian neurulation: autonomous movements of the neural plate, autonomous movements of the epidermis, and interactions in the neural plate/epidermis transition zone. *Dev. Dyn.* 204, 323–337. doi: 10.1002/aja.1002040310
- Murdoch, J. N., Damrau, C., Paudyal, A., Bogani, D., Wells, S., Greene, N. D., et al. (2014). Genetic interactions between planar cell polarity genes cause diverse neural tube defects in mice. *Dis. Model. Mech.* 7, 1153–1163. doi: 10.1242/dmm.016758
- Muto, S., Hata, M., Taniguchi, J., Tsuruoka, S., Moriwaki, K., Saitou, M., et al. (2010). Claudin-2-deficient mice are defective in the leaky and cation-selective paracellular permeability properties of renal proximal tubules. *Proc. Natl. Acad. Sci. U.S.A.* 107, 8011–8016. doi: 10.1073/pnas.0912901107
- Nakamura, S., Irie, K., Tanaka, H., Nishikawa, K., Suzuki, H., Saitoh, Y., et al. (2019). Morphologic determinant of tight junctions revealed by claudin-3 structures. *Nat. Commun.* 10:816. doi: 10.1038/s41467-019-08760-7
- Nakano, Y., Kim, S. H., Kim, H. M., Sanneman, J. D., Zhang, Y., Smith, R. J., et al. (2009). A claudin-9-based ion permeability barrier is essential for hearing. *PLoS Genet.* 5:e1000610. doi: 10.1371/journal.pgen.1000610
- Ng, P. C., and Henikoff, S. (2003). SIFT: predicting amino acid changes that affect protein function. *Nucleic Acids Res.* 31, 3812–3814. doi: 10.1093/nar/gkg509
- Nishimura, T., Honda, H., and Takeichi, M. (2012). Planar cell polarity links axes of spatial dynamics in neural-tube closure. *Cell* 149, 1084–1097. doi: 10.1016/j.cell.2012.04.021
- Nitta, T., Hata, M., Gotoh, S., Seo, Y., Sasaki, H., Hashimoto, N., et al. (2003). Size-selective loosening of the blood-brain barrier in claudin-5-deficient mice. *J. Cell Biol.* 161, 653–660. doi: 10.1083/jcb.200302070
- Paudyal, A., Damrau, C., Patterson, V. L., Ermakov, A., Formstone, C., Lalanne, Z., et al. (2010). The novel mouse mutant, chuzhoi, has disruption of Ptk7 protein and exhibits defects in neural tube, heart and lung development and abnormal planar cell polarity in the ear. *BMC Dev. Biol.* 10:87. doi: 10.1186/1471-213X-10-87
- Piontek, A., Rossa, J., Protze, J., Wolburg, H., Hempel, C., Gunzel, D., et al. (2017). Polar and charged extracellular residues conserved among barrier-forming claudins contribute to tight junction strand formation. *Ann. N. Y. Acad. Sci.* 1397, 143–156. doi: 10.1111/nyas.13341
- Piontek, J., Winkler, L., Wolburg, H., Muller, S. L., Zuleger, N., Piehl, C., et al. (2008). Formation of tight junction: determinants of homophilic interaction between classic claudins. *FASEB J.* 22, 146–158. doi: 10.1096/fj.07-8319com
- Robertson, S. L., Smedley, J. G. III, Singh, U., Chakrabarti, G., Van Itallie, C. M., Anderson, J. M., et al. (2007). Compositional and stoichiometric analysis of *Clostridium perfringens* enterotoxin complexes in Caco-2 cells and claudin 4 fibroblast transfectants. *Cell Microbiol.* 9, 2734–2755. doi: 10.1111/j.1462-5822.2007.00994.x
- Robinson, A., Escuin, S., Doudney, K., Vekemans, M., Stevenson, R. E., Greene, N. D., et al. (2012). Mutations in the planar cell polarity genes CELSR1 and SCRIB are associated with the severe neural tube defect craniorachischisis. *Hum. Mutat.* 33, 440–447. doi: 10.1002/humu.21662
- Robinson, J. T., Thorvaldsdottir, H., Wenger, A. M., Zehir, A., and Mesirov, J. P. (2017). Variant review with the integrative genomics viewer. *Cancer Res.* 77, e31–e34. doi: 10.1158/0008-5472.Can-17-0337
- Robinson, J. T., Thorvaldsdottir, H., Winckler, W., Guttman, M., Lander, E. S., Getz, G., et al. (2011). Integrative genomics viewer. *Nat. Biotechnol.* 29, 24–26. doi: 10.1038/nbt.1754
- Rolo, A., Skoglund, P., and Keller, R. (2009). Morphogenetic movements driving neural tube closure in *Xenopus* require myosin IIB. *Dev. Biol.* 327, 327–338. doi: 10.1016/j.ydbio.2008.12.009
- Rossa, J., Ploeger, C., Vorreiter, F., Saleh, T., Protze, J., Gunzel, D., et al. (2014). Claudin-3 and claudin-5 protein folding and assembly into the tight junction are controlled by non-conserved residues in the transmembrane 3 (TM3) and extracellular loop 2 (ECL2) segments. *J. Biol. Chem.* 289, 7641–7653. doi: 10.1074/jbc.m113.531012
- Rossi, A., Biancheri, R., Cama, A., Piatelli, G., Ravegnani, M., and Tortori-Donati, P. (2004). Imaging in spine and spinal cord malformations. *Eur. J. Radiol.* 50, 177–200. doi: 10.1016/j.ejrad.2003.10.015
- Sausedo, R. A., Smith, J. L., and Schoenwolf, G. C. (1997). Role of nonrandomly oriented cell division in shaping and bending of the neural plate. *J. Comp. Neurol.* 381, 473–488. doi: 10.1002/(sici)1096-9861(19970519)381:4<473::aid-cne7>3.0.co;2-#
- Schoenwolf, G. C. (1991). Cell movements driving neurulation in avian embryos. *Dev. Suppl.* 2, 157–168.
- Schoenwolf, G. C., and Alvarez, I. S. (1989). Roles of neuroepithelial cell rearrangement and division in shaping of the avian neural plate. *Development* 106, 427–439.

- Schoenwolf, G. C., Folsom, D., and Moe, A. (1988). A reexamination of the role of microfilaments in neurulation in the chick embryo. *Anat. Rec.* 220, 87–102. doi: 10.1002/ar.1092200111
- Schoenwolf, G. C., and Franks, M. V. (1984). Quantitative analyses of changes in cell shapes during bending of the avian neural plate. *Dev. Biol.* 105, 257–272. doi: 10.1016/0012-1606(84)90284-7
- Schwarz, J. M., Rodelsperger, C., Schuelke, M., and Seelow, D. (2010). MutationTaster evaluates disease-causing potential of sequence alterations. *Nat. Methods* 7, 575–576. doi: 10.1038/nmeth0810-575
- Sherry, S. T., Ward, M. H., Kholodov, M., Baker, J., Phan, L., Smigielski, E. M., et al. (2001). dbSNP: the NCBI database of genetic variation. *Nucleic Acids Res.* 29, 308–311. doi: 10.1093/nar/29.1.308
- Simard, A., Di Pietro, E., and Ryan, A. K. (2005). Gene expression pattern of Claudin-1 during chick embryogenesis. *Gene Expr. Patterns* 5, 553–560. doi: 10.1016/j.modgep.2004.10.009
- Simard, A., Di Pietro, E., Young, C. R., Plaza, S., and Ryan, A. K. (2006). Alterations in heart looping induced by overexpression of the tight junction protein Claudin-1 are dependent on its C-terminal cytoplasmic tail. *Mech. Dev.* 123, 210–227. doi: 10.1016/j.mod.2005.12.004
- Smith, J. L., and Schoenwolf, G. C. (1987). Cell cycle and neuroepithelial cell shape during bending of the chick neural plate. *Anat. Rec.* 218, 196–206. doi: 10.1002/ar.1092180215
- Smith, J. L., Schoenwolf, G. C., and Quan, J. (1994). Quantitative analyses of neuroepithelial cell shapes during bending of the mouse neural plate. *J. Comp. Neurol.* 342, 144–151. doi: 10.1002/cne.903420113
- Stevenson, B. R., Heintzelman, M. B., Anderson, J. M., Citi, S., and Mooseker, M. S. (1989). ZO-1 and cingulin: tight junction proteins with distinct identities and localizations. *Am. J. Physiol.* 257(4 Pt 1), C621–C628.
- Stevenson, B. R., Siliciano, J. D., Mooseker, M. S., and Goodenough, D. A. (1986). Identification of ZO-1: a high molecular weight polypeptide associated with the tight junction (zonula occludens) in a variety of epithelia. *J. Cell Biol.* 103, 755–766. doi: 10.1083/jcb.103.3.755
- Suzuki, H., Nishizawa, T., Tani, K., Yamazaki, Y., Tamura, A., Ishitani, R., et al. (2014). Crystal structure of a claudin provides insight into the architecture of tight junctions. *Science* 344, 304–307. doi: 10.1126/science.1248571
- Tamura, A., Kitano, Y., Hata, M., Katsuno, T., Moriwaki, K., Sasaki, H., et al. (2008). Megaintestine in claudin-15-deficient mice. *Gastroenterology* 134, 523–534. doi: 10.1053/j.gastro.2007.11.040
- Tanaka, M., Kamata, R., and Sakai, R. (2005). EphA2 phosphorylates the cytoplasmic tail of Claudin-4 and mediates paracellular permeability. *J. Biol. Chem.* 280, 42375–42382. doi: 10.1074/jbc.m503786200
- Thorvaldsdottir, H., Robinson, J. T., and Mesirov, J. P. (2013). Integrative Genomics Viewer (IGV): high-performance genomics data visualization and exploration. *Brief Bioinform.* 14, 178–192. doi: 10.1093/bib/bbs017
- Ting, S. B., Wilanowski, T., Auden, A., Hall, M., Voss, A. K., Thomas, T., et al. (2003). Inositol- and folate-resistant neural tube defects in mice lacking the epithelial-specific factor Grhl-3. *Nat. Med.* 9, 1513–1519. doi: 10.1038/nm961
- Van Itallie, C. M., Aponte, A., Tietgens, A. J., Gucek, M., Fredriksson, K., and Anderson, J. M. (2013). The N and C termini of ZO-1 are surrounded by distinct proteins and functional protein networks. *J. Biol. Chem.* 288, 13775–13788. doi: 10.1074/jbc.m113.466193
- Wallingford, J. B., and Harland, R. M. (2002). Neural tube closure requires Dishevelled-dependent convergent extension of the midline. *Development* 129, 5815–5825. doi: 10.1242/dev.00123
- Wang, J., Hamblet, N. S., Mark, S., Dickinson, M. E., Brinkman, B. C., Segil, N., et al. (2006). Dishevelled genes mediate a conserved mammalian PCP pathway to regulate convergent extension during neurulation. *Development* 133, 1767–1778. doi: 10.1242/dev.02347
- Wang, Y., Guo, N., and Nathans, J. (2006). The role of Frizzled3 and Frizzled6 in neural tube closure and in the planar polarity of inner-ear sensory hair cells. *J. Neurosci.* 26, 2147–2156. doi: 10.1523/jneurosci.4698-05.2005
- Wang, M., Marco, P., Capra, V., and Kibar, Z. (2019). Update on the Role of the Non-Canonical Wnt/planar cell polarity pathway in neural tube defects. *Cells* 8:198. doi: 10.3390/cells8101198
- Wang, Y., Thekdi, N., Smallwood, P. M., Macke, J. P., and Nathans, J. (2002). Frizzled-3 is required for the development of major fiber tracts in the rostral CNS. *J. Neurosci.* 22, 8563–8573.
- Yamaguti, P. M., Neves, F. A., Hotton, D., Bardet, C., de La Dure-Molla, M., Castro, L. C., et al. (2017). Amelogenesis imperfecta in familial hypomagnesaemia and hypercalciuria with nephrocalcinosis caused by CLDN19 gene mutations. *J. Med. Genet.* 54, 26–37. doi: 10.1136/jmedgenet-2016-103956
- Yao, F., Kausalya, J. P., Sia, Y. Y., Teo, A. S., Lee, W. H., Ong, A. G., et al. (2015). Recurrent Fusion Genes in Gastric Cancer: CLDN18-ARHGAP26 induces loss of epithelial integrity. *Cell Rep.* 12, 272–285.
- Ybot-Gonzalez, P., Savery, D., Gerrelli, D., Signore, M., Mitchell, C. E., Faux, C. H., et al. (2007). Convergent extension, planar-cell-polarity signalling and initiation of mouse neural tube closure. *Development* 134, 789–799. doi: 10.1242/dev.000380
- Yu, Z., Lin, K. K., Bhandari, A., Spencer, J. A., Xu, X., Wang, N., et al. (2006). The Grainyhead-like epithelial transactivator Get-1/Grhl3 regulates epidermal terminal differentiation and interacts functionally with LMO4. *Dev. Biol.* 299, 122–136. doi: 10.1016/j.ydbio.2006.07.015
- Zaganjor, I., Sekkarie, A., Tsang, B. L., Williams, J., Razzaghi, H., Mulinare, J., et al. (2016). Describing the prevalence of neural tube defects worldwide: a systematic literature review. *PLoS One* 11:e0151586. doi: 10.1371/journal.pone.0151586

Conflict of Interest: The authors declare that the research was conducted in the absence of any commercial or financial relationships that could be construed as a potential conflict of interest.

Copyright © 2020 Baumholtz, De Marco, Capra and Ryan. This is an open-access article distributed under the terms of the Creative Commons Attribution License (CC BY). The use, distribution or reproduction in other forums is permitted, provided the original author(s) and the copyright owner(s) are credited and that the original publication in this journal is cited, in accordance with accepted academic practice. No use, distribution or reproduction is permitted which does not comply with these terms.